

Gravitational Waveform: A Tale of Two Formalisms

Donato Bini,^{1,2} Thibault Damour,³ Stefano De Angelis,⁴
Andrea Geralico,¹ Aidan Herderschee,⁵ Radu Roiban,⁶ and Fei Teng⁶

¹*Istituto per le Applicazioni del Calcolo M. Picone, CNR, I-00185 Rome, Italy*

²*INFN, Sezione di Roma Tre, I-00146 Rome, Italy*

³*Institut des Hautes Etudes Scientifiques, 91440 Bures-sur-Yvette, France*

⁴*Institut de Physique Théorique, CEA, CNRS, Université Paris-Saclay, F-91191 Gif-sur-Yvette cedex, France*

⁵*Institute for Advanced Study, Princeton, NJ 08540, USA*

⁶*Institute for Gravitation and the Cosmos, Pennsylvania State University, University Park, PA 16802, USA*

(Dated: February 12, 2024)

We revisit the quantum-amplitude-based derivation of the gravitational waveform emitted by the scattering of two spinless massive bodies at the third order in Newton's constant, $h \sim G + G^2 + G^3$ (one-loop level), and correspondingly update its comparison with its classically-derived multipolar-post-Minkowskian counterpart. A spurious-pole-free reorganization of the one-loop five-point amplitude substantially simplifies the post-Newtonian expansion. We find complete agreement between the two results up to the fifth order in the small velocity expansion after taking into account three subtle aspects of the amplitude derivation: (1) in agreement with [arXiv:2312.07452 [hep-th]], the term quadratic in the amplitude in the observable-based formalism [JHEP **02**, 137 (2019)] generates a frame rotation by half the classical scattering angle; (2) the dimensional regularization of the infrared divergences of the amplitude introduces an additional $(d-4)/(d-4)$ finite term; and (3) zero-frequency gravitons are found to contribute additional terms both at order $h \sim G^1$ and at order $h \sim G^3$ when including disconnected diagrams in the observable-based formalism.

I. INTRODUCTION

The remarkable detection of gravitational waves by the LIGO and Virgo collaborations [1, 2] sparked the development of novel quantum field theory (QFT)-based approaches to the general relativistic two-body problem which build on enormous advances in scattering amplitudes and effective field theory. The scattering regime at large minimum separation is a theoretical environment free of many subtleties related to the definition of initial and final states, making it the ideal ground for thorough comparison and cooperation with the well-tested traditional analytical approaches to this problem. In this paper we revisit such a comparison between the amplitudes-based prediction in the observable-based (KMOC) formalism [3, 4] for the classical gravitational wave signal from the scattering of two non-spinning masses and the corresponding waveform derived within the Multipolar-post-Minkowskian (MPM) formalism [5–7].

A natural framework for discussing classical scattering from the QFT perspective consists in taking the classical limit ($\hbar \rightarrow 0$) of the perturbative QFT expansion of scattering amplitudes, which is an expansion in powers of $\frac{Gm_1m_2}{Jc}$, where J is the orbital angular momentum. By collecting the appropriate terms contributing to classical observables, one should obtain the classical post-Minkowskian (PM) expansion (in powers of Newton's constant G) of the considered classical observable (e.g. an impulse, Δp^μ , or the waveform $h_{\mu\nu} \equiv g_{\mu\nu} - \eta_{\mu\nu}$). For pioneering computations of the classical PM expansion of scattering observables, see [8, 9] (waveform) and [10, 11] (impulse). Classical bodies are treated as point particles with additional properties encoded in higher-dimension operators extending their minimal interactions

with gravity. The classical limit is identified in the spirit of the correspondence principle, and Lorentz invariance of standard QFT perturbation theory facilitates keeping the complete dependence on the velocity of particles at every order in the G expansion.

Extensive effort, utilizing advances in scattering amplitude methods such as of generalized unitarity [12–16], the double-copy relations [17–19] and powerful integration methods [20–27] and complemented by worldline approaches [28, 29], explored and evaluated inclusive scattering observables for interactions of spinning and spinless bodies, such as scattering angles, impulse, etc., to remarkably high perturbative orders [30–34]. Similarly, position-dependent (point-like) observables such as the gravitational waveform emitted during a weak-field scattering process have been discussed from different perspectives and approaches [4, 35–37]. Recently, aspects of radiation and reaction were discussed in KMOC formalism at the third order in Newton's constant in [38] and the scattering waveform, $h_{\mu\nu} \sim G^1 + G^2 + G^3 + \dots$, was constructed to this order for spinless particles [39–41] (see also [42]), for spinning particles at $O(G^2)$ [43–45] and at $O(G^3)$ [46] and various orders in spin.

Gravitational wave emission from gravitating binaries has been studied with traditional analytic methods over many years, with the purpose of constructing analytical-based waveforms to be used in the detection and data-analysis of gravitational wave signals. One of the most successful analytical methods for computing the GW emission from generic sources has been the (post-Newtonian-matched) Multipolar-Post-Minkowskian (MPM) formalism [5–7]. The MPM formalism has been developed over the years to a high perturbative accuracy, recently reaching the fourth post-

Newtonian (4PN) accuracy [47, 48], i.e. the $N^4\text{LO}$ level in a PN expansion (in powers of $\frac{v^2}{c^2} + \frac{Gm}{rc^2}$) beyond the leading-order quadrupole formula pioneered by Einstein [49]. This PN accuracy includes nonlinear terms of order $O(G^5)$ in $h_{\mu\nu}$.

A comparison of the MPM and amplitudes-based results [50] revealed substantial differences. Ref. [50] also pointed out a remarkable structure: if the amplitudes-based results are interpreted as being in a frame rotated by half the classical scattering angle, then the differences are dramatically reduced. The origin of this frame rotation was recently understood by Georgoudis, Heissenberg and Russo [51] in terms of a certain cut contribution pointed out by in Ref. [42], and demonstrated explicitly in a small-frequency expansion.¹

In this paper we revisit several aspects of the amplitude- and observable-based (KMOC) [4] derivation of the classical gravitational wave signal emitted during the scattering of two non-spinning masses at the NNLO order,² $h_{\mu\nu} = G^1 + G^2 + G^3$, and of the comparison of the frequency-domain result with the corresponding waveform derived within the Multipolar-post-Minkowskian formalism. We find complete agreement to the available post-Newtonian accuracy (see Secs. VIII, X and XI).

The main difficulty with carrying out the PN expansion of the amplitude-based scattering waveform stems from the severe spurious singularities exhibited by the available results [39–41]. We reorganize both the amplitude and the cut expressions so that they are written in terms of functions free of such spurious poles on the physical sheet (see App. C). This facilitates the PN expansion, which we carry out here to 3PN accuracy³, in the equatorial ($\theta = \pi/2$) plane and for the complete dependence on the azimuthal angle ϕ . We demonstrate that the frame rotation of [50] is equivalent to the connected part of the cut contribution of the KMOC formalism through this order (see Sec. IX).

Gravitons of vanishing frequency and their contributions to observables are a notoriously thorny subject, see e.g. [52]. Ignoring them in the KMOC calculation leads to differences with the MPM results already at leading order in Newton's constant (in the time-independent Coulombic field $h_{\mu\nu} = O(G)$ generated by the incoming particles). We will show that including them resolves this difference (see Sec. V A). They also have nontrivial contributions at higher orders in Newton's constant, where, through the disconnected cut contributions, they yield

terms that can be interpreted as a Bondi-Metzner-Sachs (BMS) [53, 54] supertranslation of the result with no contributions from such states (see Secs. XI and VC). This BMS supertranslation is the same one that clarifies [52] the existence of an angular momentum loss at $O(G^2)$ [55]; its importance in the amplitudes-MPM comparison was initially observed in a low-frequency expansion at the first non-universal order [51]. A last ingredient in our comparison is a subtle $O(\epsilon/\epsilon)$ contribution which originates from the graviton being described by a symmetric, traceless $(d-2) \times (d-2)$ matrix in d dimensions (see Secs. VB and X) in our (retarded-time renormalization) scheme.

We begin with a brief description of the MPM and amplitudes-based methods used to evaluate the waveforms, emphasizing the new contributions in the latter, and then proceed to detailing our comparison. We collect the list of notations used in this paper in App. A.

Note added: While this paper was being written up, we became aware of concurrent work by Georgoudis, Heissenberg and Russo, which partly overlaps with aspects of our analysis. We thank the authors for communication and coordination on the submission.

II. INTRODUCING THE MULTIPOLAR POST-MINKOWSKIAN (MPM) FORMALISM

The two transverse-traceless components

$$f_+ = \lim_{r \rightarrow \infty} (r h_+), \quad f_\times = \lim_{r \rightarrow \infty} (r h_\times) \quad (2.1)$$

of the classical, time-domain asymptotic waveform are encoded in the complex quantity

$$\begin{aligned} W(T_r, \theta, \phi) &= \frac{c^4}{4G} (f_+ - i f_\times) \\ &= \frac{c^4}{4G} \lim_{r \rightarrow \infty} \bar{m}^\mu \bar{m}^\nu r h_{\mu\nu}, \end{aligned} \quad (2.2)$$

where the normalization prefactor $\frac{c^4}{4G}$ is used to simplify the PN expansion of W .⁴ Here $T_r \simeq t - \frac{r}{c} - 2 \frac{GM}{c^3} \log \frac{r}{cb_0}$ denotes a retarded time which contains a logarithmic shift, involving an arbitrary time scale b_0 , proportional to the total center-of-mass (c.m.) mass-energy of the system, $M \equiv \frac{E}{c^2}$, while \bar{m}^μ (defined below) is a complex, null polarization vector tangent to the sphere at infinity. The MPM formalism is usually set up in the (incoming) c.m. of the system, and computes the components of the radiative multipole moments of the binary system with respect to a frame \bar{e}_0, e_x, e_y, e_z anchored on the *classical* averaged momenta

$$\bar{p}_a = \frac{1}{2} (p_a + p'_a), \quad (a = 1, 2), \quad (2.3)$$

¹ In the version 2 update of [51], this relation between the cut contribution and frame rotation was also tested to NNLO (1PN) in the PN expansion.

² In the following we will mainly refer to this as “the EFT waveform” following the nomenclature used in the original comparison of [50], but at times we will also use “the amplitudes-based waveform” and the “KMOC waveform”.

³ Ref. [50] had reached the 2.5PN accuracy for the ϕ -even part of the waveform, without incorporating the 2PN-level terms.

⁴ We indicate powers of c , or $\eta \equiv \frac{1}{c}$, when they help to understand the PN order of various quantities. Otherwise, we often set c to 1 without warning.

rather than the incoming momenta p_a . Here, p'_a are the classical outgoing momenta, differing from the incoming ones p_a by the full classical scattering angle $\chi = O(G)$. The time axis \bar{e}_0 of the c.m. frame is

$$\bar{e}_0^\mu = \frac{\bar{p}_1^\mu + \bar{p}_2^\mu}{|\bar{p}_1^\mu + \bar{p}_2^\mu|}. \quad (2.4)$$

The vector e_y lies in the spatial direction of \bar{p}_1 (i.e. the bisector between the incoming and the outgoing spatial momentum of the first particle in the c.m. frame),

$$\bar{p}_1 = E_1 \bar{e}_0 + \bar{P}_{\text{c.m.}} e_y, \quad \bar{p}_2 = E_2 \bar{e}_0 - \bar{P}_{\text{c.m.}} e_y. \quad (2.5)$$

Here, $E_a = \sqrt{m_a^2 + P_{\text{c.m.}}^2}$, and $P_{\text{c.m.}}$ is the magnitude of the spatial part of the incoming momenta. In principle, $\bar{P}_{\text{c.m.}}$ differs from $P_{\text{c.m.}}$ by $\bar{P}_{\text{c.m.}} = P_{\text{c.m.}} \cos \frac{1}{2}\chi$. However, the difference is only at the order $\chi^2 = O(G^2)$ and will be negligible in our work. The axis vector e_x is in the plane of motion and orthogonal to e_y (and oriented from particle 2 towards particle 1). It is also the direction of the relative impact parameter,

$$b_{12} = b e_x. \quad (2.6)$$

Here b is an eikonal-type impact parameter, linked to the incoming-momenta impact parameter b_{in} by $b_{\text{in}} = b \cos \frac{1}{2}\chi$, in which the difference $O(\chi^2) = O(G^2)$ is again negligible. The last spatial axis vector e_z is orthogonal to the plane of motion (and such that e_x, e_y, e_z is positively oriented). All vectors and tensors are decomposed in the frame \bar{e}_0, e_x, e_y, e_z and the angles θ, ϕ are accordingly defined, so that

$$\begin{aligned} \mathbf{n}(\theta, \phi) &= \sin \theta \cos \phi e_x + \sin \theta \sin \phi e_y + \cos \theta e_z, \\ k &= \omega(\bar{e}_0 + \mathbf{n}(\theta, \phi)), \\ \bar{m} &= \frac{1}{\sqrt{2}} \left[\partial_\theta \mathbf{n}(\theta, \phi) - \frac{i}{\sin \theta} \partial_\phi \mathbf{n}(\theta, \phi) \right]. \end{aligned} \quad (2.7)$$

Here \mathbf{n} is the spatial unit vector that characterizes the direction of the gravitational wave propagation.

The Multipolar post-Minkowskian (MPM) formalism [5–7] computes the time-domain waveform $W^{\text{MPM}}(T_r, \theta, \phi)$ as a sum over irreducible multipolar contributions, keyed by their multipole order ℓ and their spatial parity. Even-parity (radiative) multipoles are denoted U_ℓ , $\ell = 2, 3, 4, \dots$, while odd-parity ones are denoted V_ℓ , $\ell = 2, 3, 4, \dots$. It is convenient to keep track of the $\eta \equiv \frac{1}{c}$ prefactors entering the multipole expansion of the waveform emitted by a slow-motion source by writing W as

$$\begin{aligned} W^{\text{MPM}}(T_r, \theta, \phi) &= U_2 + \eta(V_2 + U_3) + \eta^2(V_3 + U_4) \\ &+ \eta^3(V_4 + U_5) + \eta^4(V_5 + U_6) \\ &+ \eta^5(V_6 + U_7) + \dots \end{aligned} \quad (2.8)$$

With this normalization, the PN expansion of each radiative multipole U_ℓ or V_ℓ starts at the Newtonian order (in the sense that the leading order (LO) value of each

multipole is expressed in terms of Newtonian-level quantities). In Eq. (2.8), each U_ℓ or V_ℓ is expressed in terms of corresponding symmetric-trace-free (STF) Cartesian tensors of order ℓ , according to

$$\begin{aligned} U_\ell(T_r, \theta, \phi) &= \frac{1}{\ell!} \bar{m}^i \bar{m}^j n^{i_1} n^{i_2} \dots n^{i_{\ell-2}} U_{i_1 i_2 \dots i_{\ell-2}}(T_r), \\ V_\ell(T_r, \theta, \phi) &= -\frac{1}{\ell!} \frac{2\ell}{\ell+1} \bar{m}^i \bar{m}^j n^c n^{i_1} n^{i_2} \dots n^{i_{\ell-2}} \\ &\times \epsilon_{cdi} V_{j i_1 i_2 \dots i_{\ell-2}}(T_r). \end{aligned} \quad (2.9)$$

The two infinite sequences of *radiative multipole moments* $U_{i_1 i_2 \dots i_\ell}(t)$, $V_{i_1 i_2 \dots i_\ell}(t)$ (where t henceforth denotes the retarded time variable T_r) fully, and uniquely, parametrize the time, and angular, dependences of any gravitational waveform. They are formally observable if we imagine surrounding the emitting system by infinitely many GW detectors located on the sphere at infinity (in the c.m. frame). Actually, only the time-dependent part of each multipole, e.g., $U_{i_1 i_2 \dots i_\ell}(t) - U_{i_1 i_2 \dots i_\ell}(t = -\infty)$, is directly observable when considering the LO $O(\frac{1}{r})$ asymptotic gravitational field at future null infinity. Perturbative computations have, however, shown that the presence of non-zero initial values $U_{i_1 i_2 \dots i_\ell}(t = -\infty) \neq 0$ of the radiative multipoles have physical effects at future null infinity at higher orders in $O(\frac{1}{r})$, via the back-scattering of gravitational waves on spacetime curvature (“tails”) [56, 57]. We will come back to this issue below.

The (post-Newtonian(PN)-matched) MPM formalism computes each (time-domain) radiative multipole moment $U_{i_1 i_2 \dots i_\ell}(t)$, $V_{i_1 i_2 \dots i_\ell}(t)$ in terms of the stress-energy tensor of the material source, $T^{\mu\nu}(x^\lambda)$, in several steps. At the end of the day, each radiative multipole at retarded time t is given by a sum of contributions involving both source variables at time t and hereditary integrals over the past behavior of the source, i.e. over times $-\infty \leq t' \leq t$. All those hereditary integrals are expressed in terms of some *source multipole moments*, of mass-type, $I_{i_1 i_2 \dots i_\ell}(t)$, and spin-type, $J_{i_1 i_2 \dots i_\ell}(t)$. Some of the hereditary integrals are linear in the source moments (“linear tails”) while others are nonlinear because they arise from nonlinear couplings between the multipole signals in the zone exterior to the source. Finally, the source moments are computed in terms of the dynamical variables of the source by using a PN-expanded approach to the gravitational field in the near zone.

To give an idea of the structure of the expressions coming out of the MPM formalism, let us display a few of the contributions to the radiative quadrupole⁵ $U_{ij}(t)$ at the fractional 2.5PN accuracy (η^5 beyond the classic Einstein

⁵ In the formulas below the angular brackets $\langle \dots \rangle$ denote a STF projection over the enclosed indices.

quadrupole formula):

$$\begin{aligned} U_{ij}(t) &= \frac{d^2 I_{ij}(t)}{dt^2} \quad (2.10) \\ &+ \frac{2GM}{c^3} \int_0^\infty d\tau I_{ij}^{(4)}(t-\tau) \left(\log \left(\frac{\tau}{2b_0} \right) + \frac{11}{12} \right) \\ &+ \frac{G}{c^5} \left(\frac{1}{7} I_{a\langle i}^{(5)} I_{j\rangle a} - \frac{5}{7} I_{a\langle i}^{(4)} I_{j\rangle a}^{(1)} - \frac{2}{7} I_{a\langle i}^{(3)} I_{j\rangle a}^{(2)} \right) + \dots \end{aligned}$$

in which $M \equiv \frac{E}{c^2}$ is the total mass-energy of the system, and one must insert the 2.5PN-accurate value of the source quadrupole $I_{ij}(t)$.

In the MPM formalism, the successive contributions indicated in Eq. (2.10) have different origins: (i) the source quadrupole moment $I_{ij}(t)$ computes (in a PN-expanded approximation) the quadrupole moment of the effective stress-energy tensor of the system, i.e. the sum of the $T_{\text{pp}}^{\mu\nu}$ of the point particles and of the effective $T_g^{\mu\nu}$ of the near-zone gravitational field (potential gravitons, plus some local retarded-field effects); (ii) the second (hereditary) term is the linear tail contribution generated by the back-scattering of quadrupolar waves on the external-zone Coulomb field $\sim \frac{GM}{r}$ generated by the total mass-energy of the system; and (iii) is an example of the several (instantaneous) nonlinear terms arising from cubic couplings between multipole moments (here quadrupole \times quadrupole coupling).

In the c.m. frame the 2.5PN-accurate source quadrupole I_{ij} has the following structure

$$\begin{aligned} I_{ij}^{\leq 2.5PN}(t) &= \nu M \left(1 + \frac{a_2}{c^2} + \frac{a_4}{c^4} - \frac{24}{7} \frac{\nu}{c^5} \frac{G^2 M^2}{r^2} \dot{r} \right) x^i x^j \\ &+ \text{terms in } x^i v^j \text{ and } v^i v^j. \quad (2.11) \end{aligned}$$

Here, $x^i(t) = x_1^i(t) - x_2^i(t)$ denotes the relative motion (in the c.m. frame), $v^i(t) = \frac{dx^i}{dt}$ is the relative velocity, $M = m_1 + m_2$ is the total mass and ν denotes the symmetric mass ratio, $\nu = m_1 m_2 / (m_1 + m_2)^2$. In addition, in order to get explicit results for the radiative moments as a function of time, one must solve the correspondingly PN-accurate equations of motion of the binary system. The latter task is aided by the existence of a rather simple quasi-Keplerian representation of the hyperbolic-like solution of the 2PN-level conservative equations of motion (to which the effect of radiation reaction, which starts at the G^2/c^5 level, must be added) [58–60].

As the asymptotic behavior of $x^i(t)$ in the incoming state is $x^i(t) \approx v_0^i t + O(\log t)$, the source quadrupole moment is found to behave as $I_{ij}(t) \approx \nu \text{STF}[v_0^i v_0^j] \left(1 + O(\frac{v_0^2}{c^2}) \right) t^2$. One then checks that all the hereditary integrals defining $U_{ij}(t)$ are convergent, and that $U_{ij}(t)$ has a nonzero value when $t \rightarrow -\infty$ of the form

$$U_{ij}(t = -\infty) = 2\nu M \text{STF}[v_0^i v_0^j] \left(1 + O\left(\frac{v_0^2}{c^2}\right) \right). \quad (2.12)$$

Note that the nonzero value of the radiative quadrupole moment at the Newtonian approximation is a simple consequence of the classic Einstein quadrupole formula saying that $U_{ij} = \frac{d^2}{dt^2} (\sum_a \text{STF}(m_a x_a^i x_a^j)) + O(\eta^2)$.

Similar results hold for all the multipole moments. Indeed, the origin of all these nonzero initial radiative multipole moments is the fact that the waveform in the infinite past is simply given by the Coulombic field of the incoming worldlines, namely

$$f_{ij}(t = -\infty, \mathbf{n}) = \sum_a 4G \left[\frac{(p_a^i p_a^j)^{\text{TT}}}{E_a - \mathbf{n} \cdot \mathbf{p}_a} \right], \quad (2.13)$$

leading to (with $n \equiv k/\omega$)

$$W(t = -\infty) = \sum_a \frac{(\bar{m} \cdot p_a)^2}{E_a - \mathbf{n} \cdot \mathbf{p}_a} = \sum_a \frac{(\bar{m} \cdot p_a)^2}{-(n \cdot p_a)}. \quad (2.14)$$

In other words, the MPM waveform necessarily incorporates the nonzero initial value, Eqs. (2.13), (2.14), given by the Coulombic field of the incoming worldlines.

Finally, after having obtained some representation of the various time-domain multipole moments, one must compute their Fourier transforms (over the retarded time variable), namely

$$\begin{aligned} U_{i_1 i_2 \dots i_\ell}(\omega) &= \int_{-\infty}^{+\infty} dt e^{i\omega t} U_{i_1 i_2 \dots i_\ell}(t), \\ V_{i_1 i_2 \dots i_\ell}(\omega) &= \int_{-\infty}^{+\infty} dt e^{i\omega t} V_{i_1 i_2 \dots i_\ell}(t). \quad (2.15) \end{aligned}$$

This leads to a Fourier-domain MPM waveform of the form

$$\begin{aligned} W^{\text{MPM}}(\omega, \theta, \phi) &\equiv U_2(\omega, \theta, \phi) \quad (2.16) \\ &+ \eta(V_2(\omega, \theta, \phi) + U_3(\omega, \theta, \phi)) \\ &+ \eta^2(V_3(\omega, \theta, \phi) + U_4(\omega, \theta, \phi)) \\ &+ \eta^3(V_4(\omega, \theta, \phi) + U_5(\omega, \theta, \phi)) \\ &+ \eta^4(V_5(\omega, \theta, \phi) + U_6(\omega, \theta, \phi)) \\ &+ \eta^5(V_6(\omega, \theta, \phi) + U_7(\omega, \theta, \phi)) + \dots \end{aligned}$$

Here, the explicit powers of $\eta = \frac{1}{c}$ indicate those associated with the LO, Newtonian value of each radiative multipole. They serve as a reminder that the knowledge of the full waveform $W^{\text{MPM}}(\omega, \theta, \phi)$ at, say, the 2.5PN accuracy requires one to know: (i) U_2 at the fractional 2.5PN accuracy (η^5); (ii) V_2 and U_3 at the fractional 2PN accuracy (η^4); (iii) V_3 and U_4 at the fractional 1.5PN accuracy (η^3); (iv) V_4 and U_5 at the fractional 1PN accuracy (η^2); (v) V_5 and U_6 at the Newtonian accuracy (because their first PN correction starts at 1PN) and, finally, (vi) V_6 and U_7 at the Newtonian accuracy.

In addition, as we are comparing the MPM waveform to the one-loop-accuracy amplitudes-based waveform, we only need to determine the $O(G)$ and $O(G^2)$ parts of the G -expansion of the waveform (in its W guise, i.e. after dividing $\lim_{r \rightarrow \infty} \bar{m}^\mu \bar{m}^\nu r h_{\mu\nu}$ by $4G$). Finally, an

MPM/EFT waveform comparison at the 2.5PN accuracy requires, on the MPM side, the knowledge of:

$$\begin{aligned}
U_2(\omega) &\sim (G + G^2)(\eta^0 + \eta^2 + \eta^3 + \eta^4 + \eta^5) \\
V_2(\omega) \text{ and } U_3(\omega) &\sim (G + G^2)(\eta^0 + \eta^2 + \eta^3 + \eta^4) \\
V_3(\omega) \text{ and } U_4(\omega) &\sim (G + G^2)(\eta^0 + \eta^2 + \eta^3) \\
V_4(\omega) \text{ and } U_5(\omega) &\sim (G + G^2)(\eta^0 + \eta^2) \\
V_5(\omega) \text{ and } U_6(\omega) &\sim (G + G^2)(\eta^0) \\
V_6(\omega) \text{ and } U_7(\omega) &\sim (G + G^2)(\eta^0). \tag{2.17}
\end{aligned}$$

The time-dependent part ($\omega \neq 0$) of each multipole starts at order G^1 . Only their static (initial) values contribute at order G^0 , as exhibited in Eq. (2.14).

In these expansions, the terms of order η^3 only arise at order G^2 and have two different origins. One origin is the linear tails which are all of the form

$$\begin{aligned}
U_\ell^{G^2\text{tail}}(t) &= \frac{2GM}{c^3} \int_0^\infty d\tau \frac{d^2}{dt^2} U_\ell^G(t - \tau) \\
&\quad \times \left(\log\left(\frac{\tau}{2b_0}\right) + \kappa_\ell \right) \\
V_\ell^{G^2\text{tail}}(t) &= \frac{2GM}{c^3} \int_0^\infty d\tau \frac{d^2}{dt^2} V_\ell^G(t - \tau) \\
&\quad \times \left(\log\left(\frac{\tau}{2b_0}\right) + \sigma_\ell \right), \tag{2.18}
\end{aligned}$$

with

$$\begin{aligned}
\kappa_\ell &= \frac{2\ell^2 + 5\ell + 4}{\ell(\ell+1)(\ell+2)} + \sum_{k=1}^{k=\ell-2} \frac{1}{k}, \\
\sigma_\ell &= \frac{\ell-1}{\ell(\ell+1)} + \sum_{k=1}^{k=\ell-1} \frac{1}{k}, \tag{2.19}
\end{aligned}$$

in the time domain, and

$$\begin{aligned}
U_\ell^{G^2\text{tail}}(\omega) &= \frac{2GM\omega}{c^3} \left(\frac{\pi}{2} + i[\log(2\omega b_0 e^{\gamma_E}) - \kappa_\ell] \right) U_\ell^G(\omega), \\
V_\ell^{G^2\text{tail}}(\omega) &= \frac{2GM\omega}{c^3} \left(\frac{\pi}{2} + i[\log(2\omega b_0 e^{\gamma_E}) - \sigma_\ell] \right) V_\ell^G(\omega), \tag{2.20}
\end{aligned}$$

in the frequency domain.

Another origin of the $G^2\eta^3$ terms exists for V_3 and U_4 . They come from quadrupole×quadrupole couplings. E.g., in U_4 there are terms of the form

$$\begin{aligned}
U_{ijkl}^{\text{II}}(t) &= \frac{G}{c^3} \left(-\frac{21}{5} I_{\langle ij} I_{kl \rangle}^{(5)} - \frac{63}{5} I_{\langle ij}^{(1)} I_{kl \rangle}^{(4)} \right. \\
&\quad \left. - \frac{102}{5} I_{\langle ij}^{(2)} I_{kl \rangle}^{(3)} \right). \tag{2.21}
\end{aligned}$$

These quadrupole×quadrupole couplings generate terms of order G^2/c^5 in U_2 (see last line in Eq. (2.10)).

On the other hand, the terms of even order in η come from PN corrections to the source multipole moments, as exemplified by the terms $\frac{a_2}{c^2} + \frac{a_4}{c^4}$ in Eq. (2.11).

III. STRUCTURE AND COMPUTATION OF THE MPM WAVEFORM

Ref. [50] computed the multipoles needed to reach the absolute $(G^1 + G^2)\eta^5$ accuracy in the even-in- ϕ projection of the waveform. Because of the planar nature (in the xy plane) of the binary motion generating the waveform, it is easily seen that a parity-even multipole U_l contains (when decomposed in $e^{im\phi}$) m values equal to $m = l, l-2, l-4$ etc. By contrast, a parity-odd multipole V_l contains $e^{im\phi}$ contributions for $m = l-1, l-3, l-5$ etc. Therefore, the even-in- ϕ projection of W^{MPM} is given, at accuracy η^5 , by U_2, V_3, U_4, V_5 , and U_6 . The latter multipoles were computed in Ref. [50], and their values in the equatorial plane ($\theta = \frac{\pi}{2}$) were displayed there.

In the present work, we complete the MPM/EFT comparison by also computing some of the multipoles contributing to the odd-in- ϕ part of the waveform. For simplicity, we focus on only two terms in the PN expansion of the odd-in- ϕ piece, namely, the terms of order $(G^1 + G^2)(\eta^1 + \eta^4)$. These terms come from the Newtonian-level terms in V_2 and U_3 , together with the corresponding tail terms (which are $G\eta^3$ smaller than the LO contribution). We present the full angular dependence of the multipoles by giving the coefficients of the decomposition of $W^{\text{MPM}}(\omega)$ in spin-weighted (with spin-weight $s = -2$) spherical harmonics (SWSH) ${}_s Y_{lm}(\theta, \phi)$, defined with the convention spelled out in an ancillary file `MPMmultipoles.nb`. For instance, denoting for clarity $s = -2$ as $\bar{2}$, and $m = -2$ as $\bar{2}$)

$$\begin{aligned}
{}_{\bar{2}} Y_{22}(\theta, \phi) &= \sqrt{\frac{5}{4\pi}} e^{2i\phi} \cos^4\left(\frac{\theta}{2}\right), \\
{}_{\bar{2}} Y_{2\bar{2}}(\theta, \phi) &= \sqrt{\frac{5}{4\pi}} e^{-2i\phi} \cos^4\left(\frac{\theta}{2}\right). \tag{3.1}
\end{aligned}$$

The (l, m) SWSH coefficients of W^{MPM} are the sum of the SWSH coefficients of U_l and V_l (respectively multiplied by η^{l-2} and η^{l-1}),

$$W_{lm}^{\text{MPM}} = \eta^{l-2} U_{lm} + \eta^{l-1} V_{lm}, \tag{3.2}$$

where the coefficients U_{lm}, V_{lm} are defined by

$$\begin{aligned}
U_l(\theta, \phi) &= \sum_{m=-l}^l U_{lm} {}_{\bar{2}} Y_{lm}(\theta, \phi), \\
V_l(\theta, \phi) &= \sum_{m=-l}^l V_{lm} {}_{\bar{2}} Y_{lm}(\theta, \phi). \tag{3.3}
\end{aligned}$$

The coefficients U_{lm}, V_{lm} can be obtained by using the orthonormality of the ${}_s Y_{lm}(\theta, \phi)$'s, e.g.

$$U_{lm} = \int \sin \theta d\theta d\phi U_l(\theta, \phi) {}_{\bar{2}} Y_{2,m}^*(\theta, \phi). \tag{3.4}$$

In the time-domain, the U_{lm} , and V_{lm} are functions of the retarded time t . When going to the frequency domain,

they are functions of ω , with, e.g.,

$$U_{lm}(\omega) = \int_{-\infty}^{+\infty} dt e^{i\omega t} U_{lm}(t). \quad (3.5)$$

In practice, the Fourier transforms of the radiative multipoles are more conveniently performed on the Cartesian representation of $U_{i_1 i_2 \dots i_l}(t)$ and $V_{i_1 i_2 \dots i_l}(t)$. As explained in Ref. [50], it is convenient to Fourier transform the first time-derivatives of each $U_{i_1 i_2 \dots i_l}(t)$ and $V_{i_1 i_2 \dots i_l}(t)$ (which vanish like $O(1/t^2)$ at $t \rightarrow -\infty$) and to divide the result by $-i\omega$. We only consider strictly positive frequencies $\omega > 0$ because the $\omega < 0$ part is determined by the reality of $U_{i_1 i_2 \dots i_l}(t)$ and $V_{i_1 i_2 \dots i_l}(t)$, while the $\omega = 0$ part is fully described by the ingoing, asymptotic waveform $W(t = -\infty)$. $W(t = -\infty)$ is exactly given by the G^0 , linearized-gravity result Eq. (2.14).

Let us illustrate the structure (and physical content) of $U_{lm}(\omega)$, and $V_{lm}(\omega)$, by focussing on the quadrupolar contribution $U_2 = \frac{1}{2} \bar{m}^i \bar{m}^j U_{ij}$ which is the only one which starts at the Newtonian order η^0 .

We have sketched in Eq. (2.10) the various contributions to $U_{ij}(t)$ which contribute at the fractional η^5 (2.5PN) level. The first term in Eq. (2.10),

$$U_{ij}^I(t) = \frac{d^2 I_{ij}(t)}{dt^2}, \quad (3.6)$$

has η^5 contributions coming both from an explicit 2.5PN contribution in the source quadrupole moment [61],

$$I_{ij}(t) \sim \text{STF} \left[\sum_a m_a x_a^i x_a^j + \eta^2 + \eta^4 + \eta^5 + \dots \right], \quad (3.7)$$

from the need to include $O(G^2/c^5)$ radiation-reaction effects [62] in the second time-derivative of the positions $x_a^i(t)$, and from the need to compute the Fourier transform along the radiation-reacted hyperbolic motions⁶.

The second term in Eq. (2.10) is the (linear) tail contribution which starts at order $G^2 \eta^3$ and reads, in the frequency domain,

$$U_{ij}^{G^2 \text{tail}}(\omega) = \frac{2GM\omega}{c^3} \times \left[\frac{\pi}{2} + i \left(\log(2\omega b_0 e^{\gamma_E}) - \frac{11}{12} \right) \right] U_{ij}^G(\omega), \quad (3.8)$$

where we recall that $M \equiv \frac{E}{c^2}$. Here b_0 is the time scale used in the MPM formalism to adimensionalize the (Coulomb-like) logarithmic divergence contained in the tail.

The last term in Eq. (2.10) is indicative of a sum of several nonlinear contributions (generated by various couplings between the multipolar waves in the zone exterior

to the system). These terms are expressed as products of derivatives of source (and gauge) multipole moments, all taken at the same retarded time t as $U_{ij}(t)$ itself. In U_{ij} at order G^2/c^5 , there are three such nonlinear contributions: (i) one bilinear in I_{ij} (U_{ij}^{II} , denoted U_{ij}^{QQ} in [50]); (ii) one bilinear in I_{ij} and the angular momentum L_k ($U_{ij}^{\text{LI}} \equiv U_{ij}^{\text{LQ}}$), and (iii) one bilinear in I_{ij} and the $\ell = 0$ $W_{i_1 \dots i_l}$ gauge moment ($U_{ij}^{\text{WI}} \equiv U_{ij}^{\text{WQ}}$):

$$U_{ij}^{\text{II+LI+WI}}(t) = \frac{G}{c^5} \left(\frac{1}{7} I_{a\langle i}^{(5)} I_{j\rangle a} - \frac{5}{7} I_{a\langle i}^{(4)} I_{j\rangle a}^{(1)} - \frac{2}{7} I_{a\langle i}^{(3)} I_{j\rangle a}^{(2)} + \dots \right). \quad (3.9)$$

Though only one power of G enters the prefactor of Eq. (3.9), $U_{ij}^{\text{II+LI+WI}}(t)$ actually starts at the level G^2 because of the high-order ($n \geq 3$) time-derivatives of the source quadrupole moment $I_{ij}(t)$ it contains. [As said in Ref. [50] there is a final hereditary term in $U_{ij}(t)$, the nonlinear memory contribution which, however, starts at order G^3 , i.e. at the two-loop order.]

When considering the frequency-domain version of U_2 , we have (at one-loop accuracy, i.e. modulo $O(G^3)$ in W)

$$U_2(\omega) = U_2^G(\omega) + U_2^{G^2}(\omega), \quad (3.10)$$

where both $U_2^G(\omega)$ and $U_2^{G^2}(\omega)$ start at Newtonian order. The PN expansions of $U_2^G(\omega)$ and $U_2^{G^2}(\omega)$ have the structure

$$U_2^G \sim \frac{GM^2\nu}{p_\infty} (1 + \eta^2 p_\infty^2 + \eta^4 p_\infty^4 + \eta^6 p_\infty^6 + \dots),$$

$$U_2^{G^2} \sim \left(\frac{GM}{bp_\infty^2} \right) \frac{GM^2\nu}{p_\infty} (1 + \eta^2 p_\infty^2 + \eta^3 p_\infty^3 + \eta^4 p_\infty^4 + \eta^5 p_\infty^5 + \eta^6 p_\infty^6 + \dots). \quad (3.11)$$

Note that $\left(\frac{GM}{bp_\infty^2} \right)$ is dimensionless (when considering that p_∞ has the dimension of a velocity) and of the order of the Newtonian scattering angle. When considering that p_∞ is a velocity, the PN expansion is encoded in powers of $\eta p_\infty = \frac{p_\infty}{c}$. The tree-level waveform W^G (being time-symmetric) contains only even powers of ηp_∞ . By contrast, the one-loop waveform W^{G^2} starts having odd powers of ηp_∞ in its fractional PN expansion at order $\eta^3 p_\infty^3$, which is the order where hereditary tail effects arise (see Eq. (3.8)). The next odd power of ηp_∞ is $\eta^5 p_\infty^5$ which contains several types of contributions coming from: (i) η^5 and radiation-reaction contributions to Eq. (3.7); (ii) fractional 1PN corrections contained in the linear tail term Eq. (3.8); and (iii) the nonlinear contributions to U_{ij} , Eq. (3.9).

Let us finally illustrate the explicit structure of the frequency-domain waveform by displaying a few important contributions at the $O(G)$ and $O(G^2)$ levels. The Fourier transform is done at the level of the once-time-differentiated, PN-expanded, Cartesian-component radiative multipoles $\frac{d}{dt} U_{i_1 i_2 \dots i_l}(t)$ and $\frac{d}{dt} V_{i_1 i_2 \dots i_l}(t)$. The

⁶ However, as explained in Ref. [50], this can be avoided by working with $\frac{d}{dt} U_{ij}^I(t)$.

time-dependence of these quantities is conveniently obtained by using the explicit quasi-Keplerian representation of the relative two-body motion (in the c.m. frame). The latter representation is naturally expressed in the e_x, e_y vectorial frame (which is anchored on the classical \bar{p}_a momenta, rather than the incoming momenta p_a). The polar coordinates r, φ of the relative motion,

$$\begin{aligned} \mathbf{x}(t) &= x(t)e_x + y(t)e_y \\ &= r(t) [\cos \varphi(t)e_x + \sin \varphi(t)e_y], \end{aligned} \quad (3.12)$$

are given as explicit functions of an (hyperbolictype) “eccentric anomaly” variable v by *quasi-Keplerian* expressions of the form

$$\begin{aligned} \bar{n}t &= e_t \sinh(v) - v + O(\eta^4), \\ r &= \bar{a}_r (e_r \cosh(v) - 1) + O(\eta^4), \\ \varphi &= 2K \arctan \left(\sqrt{\frac{e_\varphi + 1}{e_\varphi - 1}} \tanh \left(\frac{v}{2} \right) \right) + O(\eta^4). \end{aligned} \quad (3.13)$$

Here, the quasi-Keplerian quantities $\bar{n}, e_t, e_r, e_\varphi, K$ are (PN-expanded) functions of the c.m. energy and angular momentum of the binary system (see Refs. [58–60]).

The quasi-Keplerian representation Eq. (3.13) incorporates (in the conservative case) a time symmetry around $t = 0$, corresponding to the closest approach between the two bodies. The asymptotic logarithmic drift of the two worldlines is embodied in the v parametrization involving hyperbolic functions.

Inserting the (PN-expanded) quasi-Keplerian representation Eq. (3.13) in, say,

$$-i\omega U_{i_1 i_2 \dots i_l}(\omega) = \int_{-\infty}^{+\infty} dt e^{i\omega t} \frac{d}{dt} U_{i_1 i_2 \dots i_l}(t), \quad (3.14)$$

leads to integrals which can all be obtained (at the $G+G^2$ accuracy) from the master integrals (for $u > 0$)

$$\begin{aligned} \int_{-\infty}^{+\infty} dv e^{i(u \sinh(v) - \mu v)} &= \int_{-\infty}^{+\infty} \frac{dT}{\sqrt{1+T^2}} e^{iuT - i\mu \operatorname{arcsinh} T} \\ &= 2e^{\mu \frac{\pi}{2}} K_{i\mu}(u), \end{aligned} \quad (3.15)$$

$$\begin{aligned} \int_{-\infty}^{+\infty} \frac{dv}{\cosh v} e^{iu \sinh(v)} &= \int_{-\infty}^{+\infty} \frac{dT}{1+T^2} e^{iuT} \\ &= \pi e^{-u}. \end{aligned} \quad (3.16)$$

Actually, one only needs the large-eccentricity expansion (corresponding to a PM expansion in powers of G , and to an expansion in powers of μ) of the master integral Eq. (3.15).

Using these integrals, all the SWSH components of the waveform at order $G + G^2$ are expressed as linear combinations of modified Bessel functions of order 0 and 1, $K_0(u)$ and $K_1(u)$, and (starting at the 1PN fractional order) of the exponential e^{-u}/u , with argument given by the following dimensionless version of the frequency:

$$u \equiv \frac{\omega b}{p_\infty}. \quad (3.17)$$

The coefficients of $K_0(u)$, $K_1(u)$ and e^{-u}/u are (ν -dependent) polynomials in u whose degrees increase with the PN order.

As already said, when $l = 2$ the m values are only $m = +2, m = 0$, and $m = -2$.

Here is a sample of the SWSH components of the quadrupolar piece of the waveform. At order $G^1\eta^0$ we find

$$\begin{aligned} U_{22}^{G^1\eta^0} &= -\frac{GM^2\nu}{p_\infty} \frac{2\sqrt{5\pi}}{5} [(2u+1)K_0(u) + 2(u+1)K_1(u)], \\ U_{20}^{G^1\eta^0} &= -\frac{GM^2\nu}{p_\infty} \frac{\sqrt{30\pi}}{15} K_0(u), \\ U_{2\bar{2}}^{G^1\eta^0} &= \frac{GM^2\nu}{p_\infty} \frac{2\sqrt{5\pi}}{5} [(2u-1)K_0(u) - 2(u-1)K_1(u)]. \end{aligned} \quad (3.18)$$

At order $G^1\eta^2$ we have

$$\begin{aligned} U_{22}^{G^1\eta^2} &= \frac{\nu GM^2 p_\infty \sqrt{5\pi}}{105} \left\{ [(-72\nu+38)u^2 + (-36\nu-2)u - 24\nu + 78]K_0(u) \right. \\ &\quad \left. + [(-72\nu+38)u^2 + (-72\nu+17)u - 48\nu - 138]K_1(u) \right\}, \\ U_{20}^{G^1\eta^2} &= \nu GM^2 p_\infty \frac{\sqrt{30\pi}}{105} [(-8\nu+26)K_0(u) + u(-16\nu+59)K_1(u)], \\ U_{2\bar{2}}^{G^1\eta^2} &= \frac{\nu GM^2 p_\infty \sqrt{5\pi}}{105} \left\{ [(-72\nu+38)u^2 + (36\nu+2)u - 24\nu + 78]K_0(u) \right. \\ &\quad \left. + [(72\nu-38)u^2 + (-72\nu+17)u + 48\nu + 138]K_1(u) \right\}. \end{aligned} \quad (3.19)$$

The $O(G^2\eta^0)$ multipoles have a simple relation to the $O(G^1\eta^0)$ ones:

$$U_{2m}^{G^2\eta^0} = \frac{\pi}{2} \frac{GM}{bp_\infty^2} u U_{2m}^{G^1\eta^0}. \quad (3.20)$$

Proceeding to $O(G^2\eta^2)$, we have instead

$$\begin{aligned} U_{22}^{G^2\eta^2} &= -\frac{G^2 M^3 \nu \pi^{3/2} \sqrt{5}}{210 b p_\infty} \left\{ u[u^2(72\nu - 38) + u(78\nu - 124) + 45\nu - 141] K_0(u) \right. \\ &\quad \left. + u[u^2(72\nu - 38) + u(114\nu - 143) + 90\nu + 12] K_1(u) + \frac{252(2u^2 + 2u + 1)}{u} e^{-u} \right\}, \\ U_{20}^{G^2\eta^2} &= -\frac{G^2 M^3 \nu \pi^{3/2} \sqrt{30}}{210 b p_\infty} \left[u(-47 + 15\nu) K_0(u) + u^2(-59 + 16\nu) K_1(u) \right], \\ U_{2\bar{2}}^{G^2\eta^2} &= \frac{G^2 M^3 \nu \pi^{3/2} \sqrt{5}}{210 b p_\infty} \left\{ -u[u^2(72\nu - 38) + u(-78\nu + 124) + 45\nu - 141] K_0(u) \right. \\ &\quad \left. + u[u^2(72\nu - 38) + u(-114\nu + 143) + 90\nu + 12] K_1(u) + \frac{252}{u} e^{-u} \right\}. \end{aligned} \quad (3.21)$$

At 2PN the structure of $U_2^{G^2\eta^4}$ is similar to that of $U_2^{G^2\eta^2}$ apart from a quadratic-in- ν dependence of the coefficients and an overall multiplication by p_∞^2 .

Let us finally focus on the $G^2\eta^5$ contribution to U_2 . Following the decomposition presented above, each lm component of U_2 is the sum of two terms: (i) an “instantaneous” contribution, U_{2m}^{inst} , defined as

$$U_{2m}^{\text{inst}} = U_{2m}^I + U_{2m}^{\text{II}} + U_{2m}^{\text{LI}} + U_{2m}^{\text{WI}}, \quad (3.22)$$

i.e. the sum of the source-moment-related term, U_{2m}^I , Eq. (3.7), and of the nonlinear terms indicated in Eq. (3.9); and (ii) a (nonlocal in time) tail term U_{2m}^{tail} , Eq. (3.8) (here projected on its $G^2\eta^5$ contribution). They are respectively given by:

$$\begin{aligned} U_{22}^{\text{inst} G^2\eta^5} &= \frac{2G^2 M^3 \nu^2 \sqrt{5\pi} p_\infty^2}{525b} iu \left[2(245u^2 - 57u - 15) K_0(u) + (490u^2 + 131u - 72) K_1(u) \right], \\ U_{20}^{\text{inst} G^2\eta^5} &= \frac{2G^2 M^3 \nu^2 \sqrt{30\pi} p_\infty^2}{105b} iu \left[-2K_0(u) + 29u K_1(u) \right], \\ U_{2\bar{2}}^{\text{inst} G^2\eta^5} &= \frac{2G^2 M^3 \nu^2 \sqrt{5\pi} p_\infty^2}{525b} iu \left[2(245u^2 + 57u - 15) K_0(u) - (490u^2 - 131u - 72) K_1(u) \right], \end{aligned} \quad (3.23)$$

and

$$\begin{aligned} U_{22}^{\text{tail} G^2\eta^5} &= -\frac{2}{105} \frac{G^2 M^3 \nu \sqrt{5\pi} p_\infty^2}{b} \left(i \log(2b_0 \omega e^{\gamma_E}) - i \frac{11}{12} + \frac{\pi}{2} \right) u \left\{ [(72\nu - 38)u^2 + (78\nu + 2)u + 45\nu - 78] K_0(u) \right. \\ &\quad \left. + [(72\nu - 38)u^2 + (114\nu - 17)u + 90\nu + 138] K_1(u) \right\}, \\ U_{20}^{\text{tail} G^2\eta^5} &= -\frac{2}{105} \frac{G^2 M^3 \nu \sqrt{30\pi} p_\infty^2}{b} \left(i \log(2b_0 \omega e^{\gamma_E}) - i \frac{11}{12} + \frac{\pi}{2} \right) u \left[(15\nu - 26) K_0(u) + u(16\nu - 59) K_1(u) \right], \\ U_{2\bar{2}}^{\text{tail} G^2\eta^5} &= -\frac{2}{105} \frac{G^2 M^3 \nu \sqrt{5\pi} p_\infty^2}{b} \left(i \log(2b_0 \omega e^{\gamma_E}) - i \frac{11}{12} + \frac{\pi}{2} \right) u \left\{ [(72\nu - 38)u^2 + (-78\nu - 2)u + 45\nu - 78] K_0(u) \right. \\ &\quad \left. + [(-72\nu + 38)u^2 + (114\nu - 17)u - 90\nu - 138] K_1(u) \right\}. \end{aligned} \quad (3.24)$$

Let us finally give an example of the SWSH components of the ϕ -odd (and $(m_1 - m_2)$ -odd) piece of the waveform

$$\begin{aligned} V_{21}^{G^1\eta^0} &= -4i \frac{\sqrt{5\pi}}{15} \nu GM^2 \frac{m_1 - m_2}{M} u [K_0(u) + K_1(u)], \\ V_{2\bar{1}}^{G^1\eta^0} &= -4i \frac{\sqrt{5\pi}}{15} \nu GM^2 \frac{m_1 - m_2}{M} u [K_0(u) - K_1(u)], \end{aligned} \quad (3.25)$$

with

$$\begin{aligned} V_{21}^{G^2\eta^0} &= \frac{\pi}{2} \left(\frac{GM}{bp_\infty^2} \right) u V_{21}^{G^1\eta^0}, \\ V_{2\bar{1}}^{G^2\eta^0} &= \frac{\pi}{2} \left(\frac{GM}{bp_\infty^2} \right) u V_{2\bar{1}}^{G^1\eta^0}, \end{aligned} \quad (3.26)$$

as before. The corresponding tail contributions are given by

$$\begin{aligned} V_{21}^{G^2\eta^3} &= -\frac{4\sqrt{5\pi}}{15b} \frac{m_1 - m_2}{M} \left(\frac{7}{3} + \pi i - 2 \log(2b_0 e^{\gamma_E} \omega) \right) p_\infty G^2 M^3 \nu u^2 [K_0(u) + K_1(u)] \\ &= -i \frac{GM}{b} p_\infty u \left(\frac{7}{3} i + i\pi - 2i \log(2b_0 e^{\gamma_E} \omega) \right) V_{21}^{G^1\eta^0}, \\ V_{2\bar{1}}^{G^2\eta^3} &= -\frac{4\sqrt{5\pi}}{15b} \frac{m_1 - m_2}{M} \left(\frac{7}{3} + \pi i - 2 \log(2b_0 e^{\gamma_E} \omega) \right) p_\infty G^2 M^3 \nu u^2 [K_0(u) - K_1(u)] \\ &= -i \frac{GM}{b} p_\infty u \left(\frac{7}{3} + \pi i - 2i \log(2b_0 e^{\gamma_E} \omega) \right) V_{2\bar{1}}^{G^1\eta^0}. \end{aligned} \quad (3.27)$$

All the SWSH components of the waveform W^{MPM} that we computed are available in the ancillary file `MPMmultipoles.nb` attached to this paper. They reach (in W) $(G^1 + G^2)(1 + \eta^2 + \eta^3 + \eta^4 + \eta^5)$ accuracy for the even m terms, and the $(G^1 + G^2)(\eta + \eta^4)$ accuracy for the odd m terms.

IV. THE OBSERVABLE-BASED FORMALISM

Scattering waveform can also be computed using field-theory based methods. In particular, the observable-based formalism [3] relates directly final state observables with S -matrix elements in the classical limit. Before we start to introduce the formalism, we note that in field theory, it is customary to define metric perturbation as $g_{\mu\nu} = \eta_{\mu\nu} + \kappa h_{\mu\nu}$, where $\kappa^2 = 32\pi G$. It differs from $g_{\mu\nu} = \eta_{\mu\nu} + h_{\mu\nu}$ used in the MPM calculation by a factor of κ . We will stick to the field-theory convention when computing S -matrix elements. We will compensate the factor of κ when performing the Fourier transform to impact parameter space, see Eq. (4.6) below. We will also set $c = 1$ in all the field-theory related calculations.

A. General setup

The observable-based formalism [3] constructs quantum scattering observables by comparing the expectation value of the corresponding hermitian operator \mathbb{O} between the initial and final state of the scattering process

$$\langle \mathbb{O} \rangle = \langle \psi_{\text{out}} | \mathbb{O} | \psi_{\text{out}} \rangle - \langle \psi_{\text{in}} | \mathbb{O} | \psi_{\text{in}} \rangle, \quad (4.1)$$

where \mathbb{O} could be, e.g., the momentum transferred during the scattering process or the curvature at large distances. Observables are assumed to be measured at infinity, where the gravitational field is effectively free. The evaluation of the expectation value in Eq. (4.1) proceeds by constructing the final state $|\psi_{\text{out}}\rangle$ as the time-evolution of the initial state $|\psi_{\text{in}}\rangle$, $|\psi_{\text{out}}\rangle = \mathbb{S}|\psi_{\text{in}}\rangle$, and then inserting a complete set of final states next to \mathbb{O} .

The result is an expression of $\langle \mathbb{O} \rangle$ in terms products of S -matrix elements suitably integrated over the final-state phase space.

For the scattering problem, we construct the initial two-particle states as the tensor product of two localized single-particle states,

$$\begin{aligned} |\psi_{\text{in}}\rangle &= \int d\Phi_{p_1} d\Phi_{p_2} \varphi(p_1) \varphi(p_2) e^{-i(p_1 \cdot b_1 + p_2 \cdot b_2)} |p_1 p_2\rangle, \\ d\Phi_p &= \frac{d^4 p}{(2\pi)^4} \Theta(p^0) (2\pi) \delta(p^2 + m^2), \end{aligned} \quad (4.2)$$

where the measure $d\Phi_p$ imposes the on-shell condition, and the wavepacket is normalized as $\int d\Phi_p |\varphi(p)|^2 = 1$.

To compute the scattering waveform we may choose the operator \mathbb{O} to either be the linearized Riemann tensor⁷ or to be the transverse-traceless components of the asymptotic metric fluctuations about Minkowski space at infinity. In the former approach, the metric is extracted from the expectation value of the asymptotic Newman-Penrose scalar $\Psi_4 \propto \ddot{f}_+ - i \ddot{f}_\times$, by integrating twice over time and determining the two integration constants from physical considerations. One integration constant is fixed by the boundary condition $\lim_{t \rightarrow \infty} \dot{f}(t) \sim t^{-2}$. The other corresponds to the EFT analog of the Coulombic field in Eq. (2.13).

The latter choice yields directly the waveform. It also gives a matrix-element interpretation of the integration constants needed to reconstruct the asymptotic

⁷ The linearization is a consequence of the operator being inserted in the final state, i.e. at infinity. The LSZ reduction then projects out all Green's functions with more than a single graviton.

metric from the Newman-Penrose scalar. In particular, the integration constant that is time-independent is determined by the parts of Eq. (4.1) that have support only on vanishing outgoing-graviton frequency ω . Such $\delta(\omega)$ -supported matrix elements yield nontrivial time-dependent contributions to the waveform at higher orders in G through iteration, as we will see in Sec. V C.

The observable-based formalism yields final-state observables in the complete quantum theory. The building block of the momentum-space expectation value of the classical asymptotic metric is

$$\begin{aligned} \mathcal{M}(\varepsilon, k, p_1, p_2, q_1, q_2) &\equiv i\langle p_3 p_4 | \hat{a}(k) \mathbb{T} | p_1 p_2 \rangle + \langle p_3 p_4 | \mathbb{T}^\dagger \hat{a}(k) \mathbb{T} | p_1 p_2 \rangle \\ &= i\langle p_3 p_4 k | \mathbb{T} | p_1 p_2 \rangle + \langle p_3 p_4 | \mathbb{T}^\dagger \hat{a}(k) \mathbb{T} | p_1 p_2 \rangle, \end{aligned} \quad (4.3)$$

where \hat{a} creates a physical graviton with polarization vector ε when acting to the left. The momentum lost by each matter particle is

$$q_1 = p_1 - p_4, \quad q_2 = p_2 - p_3, \quad (4.4)$$

and momentum conservation requires that $q_1 + q_2$ be the outgoing graviton momentum k . The first term in \mathcal{M} is the five-point amplitude with one graviton in the final state; the second term is a unitarity cut that gives a particular discontinuity of the quantum amplitude. We shall refer to this bilinear-in- T term as the “unitarity cut term”, or simply, the “cut term”. The matrix element \mathcal{M} is a Lorentz invariant function of the various scalar products of $(\varepsilon, k, p_1, p_2, q_1 - q_2)$. For notational convenience, in the following we will (partially) suppress the arguments of \mathcal{M} .

The absence of local diffeomorphism-invariant observables in general relativity requires that one be careful with the effect of large gauge transformations on asymptotic observables. The asymptotic Newman-Penrose scalar and the transverse-traceless components of the asymptotic metric are invariant under decaying-at-infinity coordinate transformations, $\delta h_{\mu\nu} = \partial_{(\mu} \xi_{\nu)}$, but are not invariant under BMS transformations. However, as we will see in Section V C, both the KMOC and MPM formalisms (implicitly) use the same BMS vacuum, referred to as “intrinsic gauge” in Ref. [52].⁸

B. Classical limit

As we reviewed above, the observable-based formalism establishes the relation between observables with complete velocity dependence and the matrix element \mathcal{M} in the quantum theory. The correspondence principle,

stating that the classical regime emerges in the limit of large (macroscopic) conserved charges, provides a means to extract the classical observables from their quantum mechanical counterpart. In our case these charges are the particles’ masses, momenta and orbital angular momenta J , i.e. $J \gg \hbar = 1$ and $m \gg M_{\text{Pl}}$. It then follows [3, 63, 64] that the impact parameter b is much larger than the Compton wave length $\lambda_c = p^{-1}$ or, equivalently, that the momentum transfer q is much smaller than the typical external momenta p ⁹ and that observables are series in the effective coupling $G m_1 m_2 / J$.

In this limit, certain parts of loop-level expressions contribute to classical observables. The precise dependence on Newton’s constant G and momentum transfer follows from the observation that, like Newton’s potential itself, powers of Newton’s potential are also classical; in impact parameter space, a classical L -loop contribution is proportional $(G/b)^{L+1}$. The inclusion of outgoing (gravitational) radiation with energy ω commensurate with the momentum transfer, $\omega \sim q$, does not alter this dependence because there is no suppression for the emission of classical (gravitational) radiation. Quantum scattering amplitudes are however more singular in the large impact parameter (small transferred momentum) expansion than their classical counterparts, behaving $G^{L+1}/b^{l < L+1}$, with additional mass-dependent factors. This can be understood by recalling the structure of potential scattering in non-relativistic quantum mechanics, which at N -th order in perturbation theory contains multiple insertions of the lower-order potential. The cancellation of these classically singular (or superclassical) terms in the matrix element \mathcal{M} is a test of the calculation.

It is extremely convenient to take the classical limit as early as possible [63–65], *before* the Feynman loop integrals are evaluated, as this substantially reduces the complexity of calculations. Each of the internal graviton exchanged between matter particles should mediate a long-range interaction; thus, in this regime all loop momenta ℓ should be of the same order as the total exchanged momentum q . The method of regions [66] in dimensional regularization is a systematic method to select the classical contributions to \mathcal{M} . The integration domain is split into two regions

$$\begin{aligned} \text{Hard Region : } (q_i, k, \ell) &\rightarrow (\lambda q_i, \lambda k, \lambda^0 \ell), \\ \text{Soft Region : } (q_i, k, \ell) &\rightarrow (\lambda q_i, \lambda k, \lambda \ell), \end{aligned} \quad (4.5)$$

and the latter generates all classical terms. To evaluate an integral in only one of the regions one simply expands the integrand according to the indicated scaling in λ and

⁸ Perhaps the term “intrinsic frame” might be more appropriate as it should be possible to discern its properties through gravitational wave measurements.

⁹ In later sections we will compare MPM and amplitudes-based predictions in the PN expansion. To be in the regime of validity of both this and of the PM expansions originally used in the amplitudes computation, we must have the stronger condition on the impact parameter, $b \gg v^{-2} R_s$, corresponding to a small scattering angle $\chi \sim GM/(bv^2)$.

integrates over the *entire* integration domain. The full integral is given by the sum of the integrals in the two regions [66]; there is no overcounting because the integrand in one region yields only scaleless integrals when further expanded in the other region, and such integrals vanish in dimensional regularization.

The momentum space KMOC matrix element \mathcal{M} is related to the frequency-domain EFT waveform \mathcal{W} (here normalized as the MPM waveform W^{MPM}) through a Fourier transform to impact-parameter space,

$$\begin{aligned} \mathcal{W}(\varepsilon, k, p_1, p_2, b_1, b_2) \\ = \frac{2i}{\kappa} \int \mu(k, q_1, q_2) e^{-i(q_1 \cdot b_1 + q_2 \cdot b_2)} \mathcal{M}(\varepsilon, k, p_1, p_2, q_1, q_2), \end{aligned} \quad (4.6)$$

and we choose the (incoming) impact parameter $b_{12} = b_1 - b_2$ to be orthogonal to both p_1 and p_2 ,

$$p_1 \cdot b_{12} = p_2 \cdot b_{12} = 0. \quad (4.7)$$

The integration measure enforces momentum conservation and on-shell conditions for the matter particles. Following Eq. (4.2), we can write the measure as

$$\begin{aligned} & \int d\Phi_{p_1} d\Phi_{p_2} d\Phi_{p_3} d\Phi_{p_4} \varphi^*(p_3) \varphi^*(p_4) \varphi(p_1) \varphi(p_2) \\ & \quad \times \hat{\delta}^4(p_1 + p_2 - p_3 - p_4 - k) \\ & = \int \mu(k, q_1, q_2) + (\text{quantum}), \end{aligned} \quad (4.8)$$

and the classical contribution is

$$\begin{aligned} \mu(k, q_1, q_2) &= \frac{d^4 q_1}{(2\pi)^4} \frac{d^4 q_2}{(2\pi)^4} \hat{\delta}(2p_1 \cdot q_1) \hat{\delta}(2p_2 \cdot q_2) \\ & \quad \times \hat{\delta}^4(q_1 + q_2 - k), \end{aligned} \quad (4.9)$$

where $\hat{\delta}(x) = 2\pi\delta(x)$ and $\hat{\delta}^d(x) = (2\pi)^d\delta^d(x)$. We now sketch the derivation of Eq. (4.9). In the classical limit, the Compton wavelength ℓ_c is much smaller than the spread of the wavepacket ℓ_ϕ in the position space, which is in turn much smaller than the impact parameter $|b_1 - b_2|$, namely, $\ell_c \ll \ell_\phi \ll |b_1 - b_2|$. Consequently, in a classical scattering process, the wavepackets $\varphi(p_1)$ and $\varphi^*(p_4)$ exactly overlap up to quantum corrections, which allows us to integrate out the wavepackets, $\int d\Phi_{p_1} \varphi(p_1) \varphi^*(p_4) \simeq 1$ [same for $\varphi(p_2)$ and $\varphi^*(p_3)$]. Then in $d\Phi_{p_3}$ and $d\Phi_{p_4}$ we change the variables to q_1 and q_2 while keeping only the leading term in the on-shell condition,

$$\begin{aligned} \delta(p_4^2 + m_1^2) &\simeq \delta(2p_1 \cdot q_1), \\ \delta(p_3^2 + m_2^2) &\simeq \delta(2p_2 \cdot q_2). \end{aligned} \quad (4.10)$$

Note that we can drop the positive energy constraint in the measure because it is already implicit in the above delta function constraints.

C. IR divergence and time shift

The matrix element \mathcal{M} is infrared-divergent [38–42], with contributions from both terms in Eq. (4.3), which we regularize in dimensional regularization with $d = 4 - 2\epsilon$. Even at the one-loop order we are focusing on, the finite waveform integrand depends on whether internal states are four- or d -dimensional. This is in contrast with scattering angle calculations, where this subtlety appears only at $O(G^4)$ [31], and is due here to the presence of divergences which are effectively (additively) renormalized. To avoid possible issues probably due to unconventional forms of dimensional regularization (see e.g. [67, 68]), we use conventional dimensional regularization (CDR) [69], where all states and momenta are uniformly continued to $d = 4 - 2\epsilon$ dimensions. In the final expressions we restrict the external momenta to be four dimensional and use special four-dimensional relations such as vanishing Gram determinants for further simplifications. This regularization scheme was important in the comparison of the $O(G^4)$ scattering angle [31] and the corresponding post-Newtonian calculations of Ref. [70]; this will be the case here as well.

The IR divergences in \mathcal{M} are due to virtual soft gravitons and are expected to exponentiate [71],

$$\mathcal{M} = \exp \left[-i\omega \frac{GE}{\epsilon} (1 - \Gamma/2) \right] \mathcal{M}^{\text{fin}}, \quad (4.11)$$

where \mathcal{M}^{fin} is IR-finite but dependent of ϵ . The first term in the exponent originates from the Weinberg soft factor from the five-point amplitude [71], whose proof can be generalized to all orders in the dimensional regulator. The second term comes from the cut term [42] and Γ is defined as

$$\Gamma = \frac{3y - 2y^3}{(y^2 - 1)^{3/2}}. \quad (4.12)$$

The factor ωE in the exponent of Eq. (4.11) can be written covariantly as

$$m_1 w_1 + m_2 w_2 = \omega E, \quad (4.13)$$

where w_1 and w_2 are

$$w_a = -u_a \cdot k = -\frac{p_a \cdot k}{m_a}. \quad (4.14)$$

To understand the fate of the IR divergence, it is useful to consider the time-domain waveform, which is related to the frequency-domain waveform (4.6) by the Fourier-transform

$$\mathcal{W}(t) = \int_{-\infty}^{+\infty} \frac{d\omega}{2\pi} \mathcal{W}(\omega) e^{-i\omega t}. \quad (4.15)$$

The IR divergent phase can now be absorbed in the (re)definition of the retarded time,

$$t \rightarrow t + \delta t_{\text{IR}}, \quad \delta t_{\text{IR}} = \frac{GE}{\epsilon} (1 - \Gamma/2). \quad (4.16)$$

Equivalently, we can choose to use the IR finite matrix element in Eq. (4.6) when computing the waveform,

$$\mathcal{M} \rightarrow \mathcal{M}^{\text{fin}} = \exp \left[i\omega \frac{GE}{\epsilon} (1 - \Gamma/2) \right] \mathcal{M}. \quad (4.17)$$

The result for this IR-finite matrix element at L loops depends on the $O(\epsilon^{1 \leq n \leq L})$ part of \mathcal{M} , which in turn depends on the dimensionality of the internal states at lower-loop orders. In particular, the tree-level term in \mathcal{M} contains such $O(\epsilon)$ contributions which enforce that the regularized theory contains only d -dimensional graviton states, which we will refer to as $\epsilon \mathcal{M}_{\text{extra}}^{(0)}$. While they are unimportant for the $O(G)$ waveform, they interfere with the $O(G/\epsilon)$ argument of the phase and yield finite contributions at $O(G^2)$ proportional to $\mathcal{M}_{\text{extra}}^{(0)}$. At one-loop order inclusion of these terms amounts to a choice of scheme, and the one used here is different from that used in [38–42]. Their inclusion however is natural in light of the fact that Weinberg’s exponentiation of IR divergences holds to all orders in dimensional regulator in CDR suggesting that they are required for the exponentiation at two and higher loops. Furthermore, this scheme led to a successful comparison of amplitudes and PN predictions for the $O(G^4)$ conservative scattering angle, where similar ϵ/ϵ effects played an important role.

V. WAVEFORM FROM OBSERVABLE-BASED FORMALISM

Based on their origin in the T -matrix element, we can divide momentum-space matrix element \mathcal{M} into three categories,

$$\mathcal{M}(k, q_1, q_2) = \mathcal{M}_{\text{const}}(k, q_1, q_2) + \mathcal{M}_{\text{conn}}(k, q_1, q_2) + \mathcal{M}_{\text{disc}}(k, q_1, q_2). \quad (5.1)$$

The first term $\mathcal{M}_{\text{const}}$ is contributed by matrix elements that have the external graviton attached to an on-shell three-point vertex. Due to momentum conservation, the graviton must have zero energy. Thus $\mathcal{M}_{\text{const}}$ corresponds to a constant gravitational background. The second term $\mathcal{M}_{\text{conn}}$ contains the amplitudes and unitarity cuts contributed from connected T -matrix elements with generic momentum, while $\mathcal{M}_{\text{disc}}$ contains the unitarity cuts containing disconnected T -matrix elements.

In this section, the matter momentum p_a and four-velocity u_a are to be understood as the “barred variables” in amplitude literature (see e.g. [72, 73]). They differ from the true momentum \mathbf{p}_a (used e.g. in App. D) by half of the momentum transfer q_a , i.e. $p_a = \mathbf{p}_a + q_a/2$. In the classical limit, the difference between p_a and \mathbf{p}_a is quantum so they are indistinguishable. In contrary, the \bar{p}_a used in the MPM calculation is the “(classical) averaged momentum”, defined as $\bar{p}_a = p_a + \Delta p_a/2$, where Δp_a is the classical impulse.

A. Constant background

Exactly-zero energy excitations are an interesting feature of quantum field theories with massless particles. On the one hand, the inclusion of an arbitrary number of such excitations does not change the energy of any state, such as the Higgs field in spontaneously-broken gauge theories [74, 75]. On the other, they, and their off-shell extensions, may condense into nontrivial time-independent backgrounds, such as the Coulomb field of a point charge or the Schwarzschild metric [76, 77]. From the perspective of on-shell scattering amplitudes around flat space, only the asymptotic zero-energy states appear to be relevant. It has been suggested in Ref. [78] that their effects may be incorporated in a vacuum with no such excitations through a coherent state.

It was emphasized in Ref. [52] that the constant part of the waveform is dependent on the choice of BMS supertranslation frame. The so-called “canonical frame” is defined to have a vanishing time-independent component and the “intrinsic frame” having the non-vanishing value given in Eq. (2.13). A BMS supertranslation connects the waveforms in the two frames; in light of Ref. [78] we may expect that this supertranslation is captured by coherent state of low/vanishing-energy gravitons. Instead of exploring the all-order nature of this expectation, we will study the effect of including zero-energy gravitons in the KMOC computation.

The leading order contribution to $\mathcal{M}_{\text{const}}$ comes from the diagram shown in Fig. 1a: the momentum of one matter particle is conserved while the other emits a graviton. The relevant amplitudes are

$$\mathcal{M}_3(k, p_1, p_4) = -i\kappa(\epsilon \cdot p_1)^2, \\ \mathcal{M}_3(k, p_2, p_3) = -i\kappa(\epsilon \cdot p_2)^2. \quad (5.2)$$

For on-shell and real momenta, this process is supported at the origin of phase space, at which the emitted graviton has exactly zero energy.

Since one matter particle does not participate in the scattering, we need to use the three-particle phase space to perform the Fourier transform,

$$\mathcal{W}_{\text{const}}(k) \Big|_{m_1} = \frac{2i}{\kappa} \int d\Phi_{p_4} \hat{\delta}^4(p_1 - p_4 - k) e^{-i(p_1 - p_4) \cdot b_1} \\ \times \mathcal{M}_3(k, p_1, p_4) \\ = m_1(\epsilon \cdot u_1)^2 \hat{\delta}(u_1 \cdot k). \quad (5.3)$$

It is easy to see by going to the rest frame of the particle of mass m_1 that the delta function has a unique solution for which the graviton has exactly zero energy.

Thus, if exactly zero energy gravitons are excluded from the spectrum of states, $\mathcal{W}_{\text{const}}(k) = 0$ and we recover the expected result in the BMS canonical frame. Consistently excluding such gravitons from higher-order calculations amounts to excluding all kinematic configurations which constrain at least one graviton to have exactly zero energy.

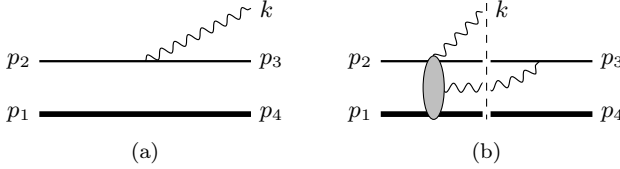


FIG. 1. The contribution to the KMOC matrix element from the disconnected components of the T -matrix.

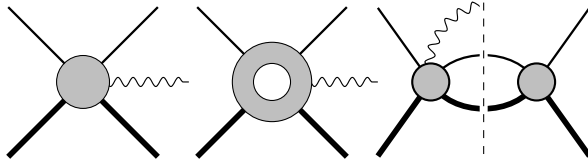


FIG. 2. The connected contribution to the KMOC matrix element. Each blob here is a connected component of the T -matrix. The first two graphs are respectively the tree and one-loop amplitude, and the last graph is a unitarity cut. The external particles are labeled in the same way as Fig. 1.

Conversely, allowing such contributions reproduces the MPM Coulombic background given in Eqs. (2.13) and (2.14).¹⁰¹¹ At higher orders, it requires us to consistently include special kinematic configurations localizing at least one graviton at the origin of phase space. Furthermore, we may expect that these terms may be obtained from those supported on finite-energy configurations through the same supertranslation as the one connecting the intrinsic and canonical frames.

As we have discussed in Sec. IV A, the Coulombic background serves to fix the initial value of the waveform. Since the three-point amplitudes are sufficient to match the initial condition with the MPM calculation, other diagrams involving a zero energy graviton are not expected to contribute to the constant background. We will show in App. D that it is indeed the case.

B. Amplitudes and connected cuts

The contribution of all the connected (generic momentum) T -matrix elements to \mathcal{M} have been evaluated

¹⁰ We note that the “constant background” here is different from $\mathcal{M}^{\text{lin}}(k)$ given in Eq. (5.2) of [50]. Here the background is chosen to be the pure time-independent piece of the waveform that is present at $t = -\infty$, while $\mathcal{M}^{\text{lin}}(k)$ there was defined as the average of the time-independent contributions at $t = \pm\infty$. In other words, $\mathcal{M}^{\text{lin}}(k)$ included some time-dependent evolutions that contribute to the gravitational-wave memory.

¹¹ The observation that zero-energy gravitons reproduce the Coulombic background was also made recently in a related context in [79].

in [38–41] to $O(\kappa^5)$. We can write it as

$$\mathcal{M}_{\text{conn}}(k, q_1, q_2) = \mathcal{M}^{\text{tree}} + \mathcal{M}^{\text{1 loop}} + \mathcal{S}^{\text{1 loop}} + O(\kappa^7), \quad (5.4)$$

where $\mathcal{M}^{\text{tree}}$ and $\mathcal{M}^{\text{1 loop}}$ are respectively the tree-level and one-loop amplitude contributed from the first term (linear in T) of Eq. (4.3), while the cut contribution $\mathcal{S}^{\text{1 loop}}$ comes from the second term of Eq. (4.3). Diagrammatically they are represented by Fig. 2.

For later convenience, we separate out the κ and mass dependence from $\mathcal{M}^{\text{tree}}$,

$$\mathcal{M}^{\text{tree}} = \kappa^3 m_1^2 m_2^2 \mathcal{M}_d^{(0)}. \quad (5.5)$$

The reduced tree-level amplitude is given by

$$\begin{aligned} \mathcal{M}_d^{(0)} = & i \left[-F_2^2 \frac{y^2}{q_1^2 q_2^2 w_2^2} \right. \\ & + F_3^2 \left(-\frac{1}{q_1^2 q_2^2} + \frac{y}{q_2^2 w_1 w_2} + \frac{y^2}{4w_1^2 w_2^2} - \frac{q_1^2 y^2}{4q_2^2 w_1^2 w_2^2} \right) \\ & + F_2 F_3 \left(-\frac{2y}{q_1^2 q_2^2 w_2} + \frac{y^2}{q_2^2 w_1 w_2^2} \right) \left. \right] \\ & + \frac{i}{d-2} \left[\frac{F_3^2 (q_1^2 - q_2^2)}{4q_2^2 w_1^2 w_2^2} + \frac{F_2^2}{q_1^2 q_2^2 w_2^2} - \frac{F_2 F_3}{q_2^2 w_1 w_2^2} \right]. \end{aligned} \quad (5.6)$$

where the graviton polarizations are encoded in the gauge invariant variables

$$F_1 = F_{\mu\nu} q_1^\mu u_1^\nu, \quad F_2 = F_{\mu\nu} q_2^\mu u_2^\nu, \quad F_3 = F_{\mu\nu} u_1^\mu u_2^\nu, \quad (5.7)$$

and $F_{\mu\nu} = k_\mu \varepsilon_\nu - k_\nu \varepsilon_\mu$ is the linearized field strength. For $d = 4 - 2\epsilon$, we have,

$$\mathcal{M}_{d=4-2\epsilon}^{(0)} = \mathcal{M}_{d=4}^{(0)} + \epsilon \mathcal{M}_{\text{extra}}^{(0)} + O(\epsilon^2), \quad (5.8)$$

where the extra dimensional contribution comes from the $\frac{1}{d-2}$ factor in Eq. (5.8),

$$\mathcal{M}_{\text{extra}}^{(0)} = \frac{i[4F_2^2 w_1^2 - 4F_2 F_3 w_1 q_1^2 + F_3^2 q_1^2 (q_1^2 - q_2^2)]}{8(q_1^2 q_2^2 w_1^2 w_2^2)}. \quad (5.9)$$

Although the external states are kept in exactly four dimensions, the ϵ dependence appears here to ensure that only graviton states propagate in $d = 4 - 2\epsilon$ dimensions.

This is a consequence of the dimensional regularization scheme we choose. Of course, we can set $d = 4$ when computing the tree-level waveform, and $\mathcal{M}_{\text{extra}}^{(0)}$ does not contribute.

Similarly, we can write the one-loop amplitude and cut contribution as

$$\begin{aligned} \mathcal{M}^{\text{one loop}} &= \kappa^5 m_1^3 m_2^2 \mathcal{M}_1^{(1)} + \kappa^5 m_1^2 m_2^3 \mathcal{M}_2^{(1)}, \\ \mathcal{S}^{\text{one loop}} &= \kappa^5 m_1^3 m_2^2 \mathcal{S}_1^{(1)} + \kappa^5 m_1^2 m_2^3 \mathcal{S}_2^{(1)}. \end{aligned} \quad (5.10)$$

The reduced one-loop amplitude $\mathcal{M}_1^{(1)}$ is given by

$$\mathcal{M}_1^{(1)} = -\frac{i w_1}{32\pi\epsilon} \mathcal{M}_{d=4}^{(0)} + \widetilde{\mathcal{M}}_1^{(1)}, \quad (5.11)$$

where the IR finite part $\widetilde{\mathcal{M}}_1^{(1)}$ is the same as Eq. (5.6) of [50]. The expression of $\widetilde{\mathcal{M}}_1^{(1)}$ can be found in App. B. We note that $\mathcal{M}_2^{(1)}$ in Eq. (5.10) can be obtained from $\mathcal{M}_1^{(1)}$ by exchanging the particle labels 1 and 2. On the other hand, the cut contribution can be written as

$$\mathcal{S}_1^{(1)} = \frac{i w_1 \Gamma}{64\pi\epsilon} \mathcal{M}_{d=4}^{(0)} + \widetilde{\mathcal{S}}_1^{(1)}, \quad (5.12)$$

where the finite part $\widetilde{\mathcal{S}}_1^{(1)}$ is given in App. B, and $\mathcal{S}_2^{(1)}$ is given by the same particle relabeling. Note that we have removed a local UV divergence from $\mathcal{S}_1^{(1)}$. Such terms do not affect the long-range interactions that we are interested in, and they are projected out by the Fourier transform to impact parameter space.

The full IR divergence of the one-loop waveform is

$$(\mathcal{M}^{1 \text{ loop}} + \mathcal{S}^{1 \text{ loop}}) \Big|_{\text{IR}} = -\frac{i\omega\kappa^2 E(2-\Gamma)}{64\pi\epsilon} \mathcal{M}_{d=4}^{\text{tree}}, \quad (5.13)$$

Following Eq. (4.17) and the discussion below, we can absorb the IR divergence into an infinite shift in the retarded time $\delta t_{\text{IR}} = \frac{GE}{\epsilon}(1 - \Gamma/2)$ to obtain the IR finite momentum-space waveform,

$$\begin{aligned} \mathcal{M}^{\text{fin}} &= \exp \left[i\omega \frac{GE}{\epsilon} (1 - \Gamma/2) \right] \mathcal{M} \\ &= \mathcal{M}^{\text{tree}} + \mathcal{M}^{1 \text{ loop}} + \mathcal{S}^{1 \text{ loop}} \\ &\quad + \frac{i\omega\kappa^2 E(2-\Gamma)}{64\pi\epsilon} \mathcal{M}^{\text{tree}} + O(\kappa^7) \\ &= \mathcal{M}^{\text{tree}} + \mathcal{M}^{1 \text{ loop fin}} + \mathcal{S}^{1 \text{ loop fin}} + O(\kappa^7). \end{aligned} \quad (5.14)$$

Crucially, the time shift introduces a term proportional to the d -dimensional tree amplitude $\mathcal{M}^{\text{tree}}$. While this term cancels the IR divergence (5.13), it brings an additional finite contribution proportional to the extra dimensional component (5.9). Organizing the finite one-loop amplitude and cut by the mass dependence,

$$\begin{aligned} \mathcal{M}^{1 \text{ loop fin}} &= \kappa^3 m_1^3 m_2^2 \mathcal{M}_1^{(1) \text{ fin}} + \kappa^3 m_1^2 m_2^3 \mathcal{M}_2^{(1) \text{ fin}}, \\ \mathcal{S}^{1 \text{ loop fin}} &= \kappa^3 m_1^3 m_2^2 \mathcal{S}_1^{(1) \text{ fin}} + \kappa^3 m_1^2 m_2^3 \mathcal{S}_2^{(1) \text{ fin}}, \end{aligned} \quad (5.15)$$

we get

$$\begin{aligned} \mathcal{M}_1^{(1) \text{ fin}} &= \widetilde{\mathcal{M}}_1^{(1)} + \frac{i w_1}{32\pi} \mathcal{M}_{\text{extra}}^{(0)}, \\ \mathcal{S}_1^{(1) \text{ fin}} &= \widetilde{\mathcal{S}}_1^{(1)} - \frac{i w_1 \Gamma}{64\pi} \mathcal{M}_{\text{extra}}^{(0)}. \end{aligned} \quad (5.16)$$

Comparing with Eqs. (5.11) and (5.12) we see that, while the divergence is removed by absorbing the $1/\epsilon$ into a time shift, this shift introduces a new contribution proportional to the extra dimensional component of the five-point tree amplitude defined in Eq. (5.8). Thus the additional terms proportional to $\mathcal{M}_{\text{extra}}^{(0)}$ come from the ϵ/ϵ

cancellation, and they are the direct consequence of the regularization scheme chosen in Sec. IV C. While at this loop order the inclusion of this term may be regarded as a scheme dependence (and was not included in previous amplitude calculations or comparisons), its presence here is justified by the expected higher-loop structure of IR divergences as well as by its importance in related contexts [31]. As we will see in Sec. VIII, its presence substantially improves the comparison between MPM and amplitudes-based results.

C. Cuts with disconnected matrix elements and BMS transformation

If zero-energy gravitons are excluded, then all cut contributions containing a three-point S-matrix element or an $n+1$ -point matrix element in the $1 \rightarrow n$ configuration vanish identically. All disconnected contributions to the cut term in Eq. (4.3) are of this type. If zero-energy gravitons are kept in the spectrum, the (albeit degenerate) three-point amplitude generates, at higher-order in Newton's constant, time-dependent terms through the cut term in this equation. The relevant contribution at one-loop order is shown in Fig. 1b; the discussion above implies that, at L loops, the six-point tree amplitude factor is replaced by the corresponding $(L-1)$ -loop six-point amplitude with no changes to the disconnected factor.¹²

The evaluation of this cut makes use of the fact that the cut massless momentum ℓ must have vanishing frequency, so only the leading soft limit of the six-point tree amplitude (the left blob of Fig. 1b) with two external gravitons of momenta k and ℓ is relevant,

$$\begin{aligned} \mathcal{M}_6(p_{1\ldots 4}, k, \ell) &\simeq -\kappa \mathcal{M}_5(p_{1\ldots 4}, k) \\ &\quad \times \left(\sum_{i=1}^4 \frac{\eta_a \varepsilon(\ell)_{\mu\nu} p_a^\mu p_a^\nu}{2\ell \cdot p_a - i\epsilon\eta_a} + \frac{\varepsilon(\ell)_{\mu\nu} k^\mu k^\nu}{2\ell \cdot k - i\epsilon} \right), \end{aligned} \quad (5.17)$$

where $\eta_a = \pm 1$ for outgoing and incoming particles, respectively, and $\mathcal{M}_5(p_{1\ldots 4}, k)$ is the five-point amplitude with one external graviton of momentum k .

Sewing Eq. (5.17) onto the disconnected five-point amplitude, we find that the four summed terms in Eq. (5.17) that involve massive matter momenta will lead to integrals of the form

$$\begin{aligned} &\int d^d \ell \hat{\delta}(u_3 \cdot \ell) \hat{\delta}(\ell^2) \Theta(\ell^0), \\ &\int d^d \ell \hat{\delta}(u_3 \cdot \ell) \hat{\delta}(\ell^2) \hat{\delta}(u_4 \cdot \ell) \Theta(\ell^0), \end{aligned} \quad (5.18)$$

¹² In the full quantum theory the three-point Green's function is UV divergent; this divergence arises from loop momenta outside the soft region, and do not contribute to the classical observables we are discussing here.

both of which are integrated to zero in $d = 4 - 2\epsilon$. Therefore, a nonzero contribution can only come from the last term in this equation, which corresponds to the soft graviton being attached to the outgoing graviton with momentum k . We can replace $\mathcal{M}_5(p_{1\dots 4}, k)$ by its classical limit given in Eq. (5.5). It then yields the following contribution to $\mathcal{M}_{\text{disc}}$ at $O(\kappa^5)$ (which makes use of the on-shell condition for the outgoing graviton):

$$\mathcal{M}_{\text{disc}} = -i\kappa^2 \mathcal{M}^{\text{tree}} [m_2^2 w_2^2 I(u_3, k) + m_1^2 w_1^2 I(u_4, k)], \quad (5.19)$$

where we used that in the classical limit $-p_{3,4} \cdot k = -p_{2,1} \cdot k + O(q^2) \simeq m_{2,1} w_{2,1}$ and $I(u_3, k)$ is defined as

$$\begin{aligned} I(u_3, k) &= \frac{1}{m_2} \int \frac{d^d \ell}{(2\pi)^d} \frac{\hat{\delta}(2u_3 \cdot \ell) \hat{\delta}(\ell^2) \Theta(\ell^0)}{2\ell \cdot k} \\ &= \frac{1}{m_2 \omega} \int \frac{d^d \ell}{(2\pi)^d} \frac{\hat{\delta}(2u_3 \cdot \ell) \hat{\delta}(\ell^2) \Theta(\ell^0)}{2\ell \cdot \hat{k}}, \end{aligned} \quad (5.20)$$

where $\hat{k} = k/\omega$, and $I(u_4, k)$ is obtained simply by relabeling. We did not include $\Theta(p_3^0 + \ell^0)$ for the matter cut line because $|\ell^0| \ll p_3^0$ so $\Theta(p_3^0 + \ell^0) = 1$. We have also suppressed the $i\epsilon$ in the propagator since it does not affect the integral. However, to properly include the zero energy graviton contribution across the cut, we need to introduce additional regularizations.

Since the zero energy graviton is supported only at the origin of phase space, we must regularize it so that this point, $|\ell| = 0$, remains in the integration domain.¹³ We may do this by relaxing the on-shell condition $u_3^2 = -1$ by introducing $u_3 \rightarrow \tilde{u}_3 = u_3 - \beta \hat{k}$ with arbitrary β . In the presence of $\hat{\delta}(\ell^2)$, this modifies the cut matter propagator to be

$$\begin{aligned} 2u_3 \cdot \ell &= (u_3 + \ell)^2 + 1 \rightarrow (\tilde{u}_3 + \ell)^2 + 1 \\ &\simeq 2u_3 \cdot \ell - 2\beta u_3 \cdot \hat{k}, \end{aligned} \quad (5.21)$$

where we dropped the term proportional to $\hat{k} \cdot \ell$ as it leads to integrals proportional the first of Eq. (5.18) and thus vanishes. We therefore consider instead the integral

$$\begin{aligned} \tilde{I}(u_3, k) &= \frac{e^{\gamma_E \epsilon}}{m_2 \omega} \int \frac{d^d \ell}{(2\pi)^d} \frac{\hat{\delta}(2u_3 \cdot \ell - 2\beta u_3 \cdot \hat{k}) \hat{\delta}(\ell^2) \Theta(\ell^0)}{2\ell \cdot \hat{k}} \\ &= \frac{\Theta(\beta)}{16\pi m_2 w_2} \left[\frac{1}{\epsilon} - \log \frac{w_2^2}{\omega^2} - \log \frac{\beta^2}{\pi} \right], \end{aligned} \quad (5.22)$$

and we keep only the $O(\epsilon^0)$ terms. The original integral $I(u_3, k)$ is recovered at $\beta = 0$. Using $\Theta(0) = \frac{1}{2}$, we get,¹⁴

$$I(u_3, k) = \frac{1}{32\pi m_2 w_2} \left[\frac{1}{\epsilon} - \log \frac{w_2^2}{\omega^2} - \log \frac{\beta^2}{\pi} \right], \quad (5.23)$$

¹³ This is analogous with the determination of the snail diagrams in quantum scattering amplitudes, see e.g. [80].

¹⁴ Alternatively, we can obtain $I(u_3, k)$ directly as a discontinuity of an off-shell triangle integral, which was computed in Eq. (C.4) of Ref. [81] (see Ref. [82] for comments on similar integrals), with the same off-shell continuation as discussed here.

where the divergent constants $\log \beta$ and $1/\epsilon$ will be absorbed by a time shift. We note that both integrals in Eq. (5.18) remain zero even if we used the above off-shell regularization.

Putting together Eqs. (5.19) and (5.23), we find that the cut in Fig. 1b gives a finite contribution $\mathcal{S}^{\text{1 loop disc}}$,

$$\begin{aligned} \mathcal{M}_{\text{disc}} &= \mathcal{S}^{\text{1 loop disc}} - i\omega G E \left[\frac{1}{\epsilon} - \log \frac{\beta^2}{\pi} \right] \mathcal{M}^{\text{tree}}, \\ \mathcal{S}^{\text{1 loop disc}} &= iG \left[m_1 w_1 \log \frac{w_1^2}{\omega^2} + m_2 w_2 \log \frac{w_2^2}{\omega^2} \right] \mathcal{M}^{\text{tree}}. \end{aligned} \quad (5.24)$$

The second term of $\mathcal{M}_{\text{disc}}$ can be removed by a time shift that supplements the one in Eq. (4.16). The first term, $\mathcal{S}^{\text{1 loop disc}}$, which may be interpreted as a direction-dependent time shift, is in fact the BMS supertranslation identified in [52] as relating the “canonical” and “intrinsic” BMS frames, thus explaining the angular momentum loss at $O(G^2)$ [55], as well as the transformation needed to relate the first nonuniversal term in the soft expansion of the amplitude-based [51, 83] and MPM waveforms [50].

We therefore see that zero-energy gravitons generate on the one hand a time-independent background metric at $O(G^0)$ (see Sec. V A) and, on the other hand, a time-dependent waveform at higher orders in G and moreover that both of them can be removed by the same BMS supertranslation that connects the intrinsic and canonical frames. This reinforces the close connection between zero-energy gravitons and the choice of BMS frame, which echoes features in the angular momentum loss calculations [52, 84, 85], and suggests that one may consistently ignore the disconnected cut contributions and restore them through the BMS transformation of Ref. [52]. It would be interesting to attempt to formulate the observable-based formalism in the “intrinsic” BMS frame in terms of a vacuum dressed with a coherent state of zero-energy gravitons in the spirit of Ref. [78]. Such a formulation, in which the contribution of zero-energy particles (and the associated subtleties) will emerge because of this dressing, may give a means to argue for an all-order connection between the disconnected cut contributions and the choice of BMS frame.

VI. PN AND SOFT EXPANSIONS OF KMOC WAVEFORM

The one-loop amplitude part of the \mathcal{M} matrix element computed in [39–41] exhibits spurious poles (SP). Some of these poles cancel manifestly when the amplitude is expanded in special kinematic limits such as at low velocity, in the soft limit, etc. However, manifesting such cancellations for general kinematic configurations is, at first sight, highly non-trivial and appears to require the use of Gram determinant and Bianchi identities among a huge number of terms. Algorithms for addressing such problems have been developed in Ref. [86] (see also Ref. [87]) and applied to the current problem in Ref. [46].

In App. C we take a different route and reorganize the one-loop five-point scattering amplitude (5.11) and the cut term to make manifest the cancellation of the spurious poles on the physical sheet. By direct inspection of Feynman integrals involving non-trivial numerators, we find combinations of the square roots and logarithms appearing in (5.11) such that they have high-order zeros in correspondence with the singularities of the rational functions multiplying them. It turns out that the same functions are sufficient to render both the amplitude and the cut contributions to \mathcal{M} free of spurious poles. Their expressions after this reorganization are

$$\begin{aligned} \mathcal{M}_1^{(1) \text{ fin}} &= \left[\frac{i w_1}{32\pi} \log \frac{w_1^2}{\mu_{\text{IR}}^2} + \frac{w_1}{32} + \frac{\Gamma w_1}{64} \right] \mathcal{M}_{d=4}^{(0)} \quad (6.1) \\ &+ \frac{i w_1}{32\pi} \mathcal{M}_{\text{extra}}^{(0)} + c_1 I_1 + c_2 I_2 + l'_q L_q + l'_w L_w \\ &+ R + l_q \log \frac{q_1^2}{q_2^2} + l_w \log \frac{w_2^2}{w_1^2} + l_y \frac{\operatorname{arccosh} y}{\sqrt{y^2 - 1}}, \end{aligned}$$

$$\begin{aligned} \mathcal{S}_1^{(1) \text{ fin}} &= \frac{i w_1 \Gamma}{64\pi} \mathcal{M}_{d=4}^{(0)} \log \frac{w_1 w_2 \mu_{\text{IR}}^2}{q_1^2 q_2^2 (y^2 - 1)} \quad (6.2) \\ &- \frac{i w_1 \Gamma}{64\pi} \mathcal{M}_{\text{extra}}^{(0)} + c_{\text{rat}} + c_{\text{ratio}} \log \frac{w_1^2 w_2^2}{q_1^2 q_2^2} \\ &+ c_y \operatorname{arccosh} y + c_q L_q + \mathcal{S}_1^{(1) \text{ local}}, \end{aligned}$$

where $\{I_1, I_2, L_q, L_w\}$ are SP-free combinations. Their explicit forms and construction are given in App. C. Here $\mathcal{S}_1^{(1) \text{ local}}$ includes all terms which have no singularities in $q_{1,2}^2$ (including $c_w L_w$) and therefore integrate to delta-function-supported terms in impact parameter space. Thus $\mathcal{S}_1^{(1) \text{ local}}$ can be ignored. The explicit expressions of the c and l coefficients in Eqs. (6.1) and (6.2) are included in the ancillary file `WaveformReorganisation.nb`.

A. Impact-parameter-space waveform

With the reorganized parts of the momentum space \mathcal{M} matrix element, we now discuss the Fourier transform (4.6) to obtain the impact-parameter-space (and frequency-space) waveform $\mathcal{W}(k, b_1, b_2)$. Here we will focus on the $\omega \neq 0$ (time-dependent) contribution up to $O(G^2)$. As $\mathcal{M}(k, q_1, q_2)$ is a function of the kinematic data of the incoming state, the waveform $\mathcal{W}(k, b_1, b_2)$ is naturally given in the incoming c.m. frame (e_0, e_1, e_2, e_3) anchored on the incoming momenta p_1 and p_2 . The unit time vector e_0 can be chosen as

$$e_0^\mu = \frac{p_1^\mu + p_2^\mu}{|p_1^\mu + p_2^\mu|}, \quad (6.3)$$

while the incoming momenta are along the e_2 direction,

$$p_1 = E_1 e_0 + P_{\text{c.m.}} e_2, \quad p_2 = E_2 e_0 - P_{\text{c.m.}} e_2, \quad (6.4)$$

where $E_a = \sqrt{P_{\text{c.m.}}^2 + m_a^2}$. Note that we can express E_a and $P_{\text{c.m.}}$ in terms of y as

$$\begin{aligned} P_{\text{c.m.}} &= \frac{m_1 m_2 \sqrt{y^2 - 1}}{E}, \\ E &= \sqrt{m_1^2 + 2y m_1 m_2 + m_2^2}. \end{aligned} \quad (6.5)$$

We then choose the impact parameter b_1 and b_2 to satisfy $\frac{E_1}{E} b_1^\mu + \frac{E_2}{E} b_2^\mu = 0$ and be orthogonal to e_0 . We define the relative transferred momentum q^μ by

$$q^\mu = q_1^\mu - \frac{E_1}{E} k^\mu = -q_2^\mu + \frac{E_2}{E} k^\mu, \quad (6.6)$$

such that the exponential factor in Eq. (4.6) becomes

$$e^{-i(q_1 \cdot b_1 + q_2 \cdot b_2)} = e^{-i q \cdot (b_1 - b_2)} = e^{-i q \cdot b_{12}}, \quad (6.7)$$

and thus \mathcal{W} depends only on b_{12} . The impact parameter b_{12} is orthogonal to both of the incoming momenta p_1 and p_2 . Thus we can choose it to be along the e_1 direction,¹⁵

$$b_{12} = b_{\text{in}} e_1. \quad (6.8)$$

The momentum k and polarization vector ε for the emitted graviton are given by

$$\begin{aligned} \tilde{\mathbf{n}}(\theta, \phi) &= \sin \theta \cos \phi e_1 + \sin \theta \sin \phi e_2 + \cos \theta e_3, \\ k &= \omega (e_0 + \tilde{\mathbf{n}}(\theta, \phi)), \\ \varepsilon &= \frac{1}{\sqrt{2}} \left[\partial_\theta \tilde{\mathbf{n}}(\theta, \phi) - \frac{i}{\sin \theta} \partial_\phi \tilde{\mathbf{n}}(\theta, \phi) \right]. \end{aligned} \quad (6.9)$$

They are formally the same as Eq. (2.7), but the polar angles here (θ, ϕ) are defined instead with respect to the spatial frame (e_1, e_2, e_3) . Therefore, the Fourier transform of $\mathcal{M}(k, q_1, q_2)$ in Eq. (4.6) now becomes

$$\begin{aligned} \text{FT}_b[f] &\equiv \int \mu \left(k, q + \frac{E_1}{E} k, -q + \frac{E_2}{E} k \right) e^{-i q \cdot b_{12}} f(q), \\ \mathcal{W}(\omega, \theta, \phi) &= \frac{2i}{\kappa} \text{FT}_b \left[\mathcal{M} \left(k, q + \frac{E_1}{E} k, -q + \frac{E_2}{E} k \right) \right]. \end{aligned} \quad (6.10)$$

The resulting impact parameter space waveform \mathcal{W} is in principle a Lorentz invariant function consisting of scalar products of $(\varepsilon, k, p_1, p_2, b_{12})$. However, performing this Fourier transform in complete generality is challenging. In the following, we will proceed in the incoming c.m. frame, such that the frequency-domain waveform is given as a function $\mathcal{W}(\omega, \theta, \phi)$, and consider its PN expansion.

B. PN expansion

For the PN expansion, we will stick to the conventions of reference [50], also already used here in sections II and III. It is an expansion in powers of the velocity parameter

$$p_\infty \equiv \sqrt{y^2 - 1}. \quad (6.11)$$

¹⁵ We note that $b_{\text{in}} = b + O(G^2)$. See the discussion below Eq. (2.6).

Here p_∞ is taken as dimensionless (i.e. we can replace $\eta = \frac{1}{c}$, used in Secs. II and III by 1).

Following Ref. [50], one rewrites the kinematic variables in terms of the expansion parameter p_∞ , and expands the integrand before computing the Fourier transform to impact-parameter space. This gives rise to a rather simple integrand whose integral can be expressed solely in terms of Bessel K functions and exponentials.

One starts by decomposing q^μ in terms of the external vectors (a covariant form of this decomposition, using u_1, u_2, b and a fourth vector orthogonal on them, was introduced in Ref. [4])

$$q^\mu = q^0 e_0^\mu + \Omega Q_x e_1^\mu + q_y e_2^\mu + \Omega Q_z e_3^\mu, \quad (6.12)$$

where $e_{1,2,3}^\mu$ denote the direction of impact parameter, of the c.m. momentum and of the orthogonal direction to the scattering plane, respectively – as defined in Section II. Moreover, Ω is the frequency of the emitted radiation rescaled by the expansion parameter:

$$\omega = \Omega p_\infty. \quad (6.13)$$

The integration over $q_{0,y}$ gives the following Jacobian:

$$\int \mu(k, q_1, q_2) e^{-iq \cdot b_{12}} = \frac{\Omega^2}{4m_1 m_2 p_\infty} \int \frac{dQ_x dQ_z}{(2\pi)^2} e^{-iuQ_x}, \quad (6.14)$$

where u is the dimensionless frequency variable

$$u \equiv \Omega b \equiv \frac{\omega b}{p_\infty}, \quad (6.15)$$

and the delta functions fix the components q^0, q_y :

$$\begin{aligned} q^0 &= -\frac{\Omega p_\infty}{E^2} (m_1^2 - m_2^2 - m_1 m_2 p_\infty \sin \theta \sin \phi), \\ q_y &= \frac{\Omega}{E^2} (m_1 \sqrt{p_\infty^2 + 1} + m_2) (m_2 \sqrt{p_\infty^2 + 1} + m_1). \end{aligned} \quad (6.16)$$

These relations correspond to Eqs. (5.9) in Ref. [50], except that the latter equations were expressed in the the barred com frame $(\bar{e}_0, e_x, e_y, e_z)$.

For completeness, let us give also the expressions of $w_{1,2}$ in the c.m. frame:

$$\begin{aligned} w_1 &= \frac{\Omega p_\infty}{E} \left[m_1 + m_2 \left(\sqrt{p_\infty^2 + 1} - p_\infty \sin \theta \sin \phi \right) \right], \\ w_2 &= \frac{\Omega p_\infty}{E} \left[m_2 + m_1 \left(\sqrt{p_\infty^2 + 1} + p_\infty \sin \theta \sin \phi \right) \right]. \end{aligned} \quad (6.17)$$

The original form of the amplitude [39–41] made it challenging to compute its PN expansion because of the presence of spurious poles, though Ref. [50] succeeded to carry out the expansion up to the 2.5PN approximation, and to evaluate the Fourier transform, thereby obtaining the EFT waveform as a function of ω, θ and ϕ . The SP-free version of the amplitude presented above significantly simplifies the task of PN-expanding the amplitude.

The leading orders of the various terms in Eq. (6.1) in a small- p_∞ expansion are

$$\begin{aligned} c_1 I_1 &\sim p_\infty^0 & l'_q L_q &\sim p_\infty^2 & R &\sim p_\infty^{-5} \\ c_2 I_2 &\sim p_\infty^{-5} & l'_w L_w &\sim p_\infty^2 & & \\ l_q \log \frac{q_1^2}{q_2^2} &\sim p_\infty^0 & l_w \log \frac{w_2^2}{w_1^2} &\sim p_\infty^2 & l_y \frac{\operatorname{arccosh} y}{\sqrt{y^2 - 1}} &\sim p_\infty^{-1}. \end{aligned} \quad (6.18)$$

Thus, in this organization three of the eight terms start contributing only at 2PN order. Moreover, the cancellation of terms $p_\infty^{n \leq -2}$ is quite straightforward to observe. This allowed us to reach the 3PN accuracy. Even though we have so far only computed the 3PN-accurate EFT waveform in the equatorial plane, i.e. when taking $\theta = \frac{\pi}{2}$, there is no technical obstacle to derive it for arbitrary values of θ . Although most integrals in Q_z and Q_x are absolutely convergent, some of the contributions from the cut term must be interpreted as Fourier transforms of tempered distributions.

As explained in [50] the PN expansion of the amplitude yields an integrand containing only integer or half-integer powers of

$$D_0 = 1 + Q_x^2 + Q_z^2, \quad (6.19)$$

with numerators polynomial in Q_z and Q_x . The Fourier transforms of all these terms are computed from the general formula

$$\int \frac{dQ_x dQ_z}{(2\pi)^2} e^{-iuQ_x} \frac{Q_x^n}{D_0^m} = \frac{i^{n2-m}}{\pi \Gamma[m]} \partial_u^n [u^{m-1} K_{m-1}(u)], \quad (6.20)$$

However, the cut terms (new with this work) involve the first power of $\log D_0$ in the numerator. Such terms can be integrated by using the formula

$$\begin{aligned} \int \frac{dQ_x dQ_z}{(2\pi)^2} e^{-iuQ_x} \frac{Q_x^n \log D_0}{D_0^m} &= \\ = -\partial_\rho \left\{ \frac{i^{n2-m-\rho}}{\pi \Gamma[m+\rho]} \partial_u^n [u^{m+\rho-1} K_{m+\rho-1}(u)] \right\} \Big|_{\rho=0}. \end{aligned} \quad (6.21)$$

involving a derivative with respect to the order of the Bessel $K_\nu(u)$ (around an integer value of ν).

The final result can be further reduced using relations among modified Bessel functions of the second kind to linear combinations of $K_0(u)$, $K_1(u)$ and e^{-u} with coefficients that are rational functions of u . The results of this expansion up to 3PN order are presented in the ancillary file `PNExpandedEFT.nb`.¹⁶

¹⁶ For the analysis of the PN expansion of the various terms contributing to the amplitudes, we refer to Section V of Ref. [50].

C. Soft-graviton expansion

We also computed the soft-graviton expansion of the waveform in impact parameter space:¹⁷

$$\mathcal{W} \simeq \frac{\mathcal{A}}{\omega} + \mathcal{B} \log \omega + \mathcal{C} \omega (\log \omega)^2 + \mathcal{D} \omega \log \omega. \quad (6.22)$$

Care must be taken when carrying out the soft-graviton expansion at the level of the waveform integrand. As one quickly discovers, a naive expansion leads to uncontrolled infrared divergences at sufficiently high orders in the subsequent Fourier transform in momentum transfer at sufficiently high orders.

Thus, the soft-graviton expansion is intertwined with the Fourier transform to impact parameter space. The presence of the small parameter ω indicates that the appropriate framework for the evaluation of the latter is the method of regions.¹⁸ There are two distinct contributing regions, $q_1 \rightarrow \omega^0 q_1$ and $q_1 \rightarrow \omega q_1$, and each of them has a different small- ω expansion which must be added to obtain the correct result. In both regions the resulting integrals can be evaluated in closed form, as done in Ref. [4].

The soft-graviton expansion corresponds to the large time expansion of the time-domain waveform. The behavior of the scattering waveform in this regime exhibits universality as emphasized in Refs. [89, 90]. In particular, when expressed in terms of the incoming and outgoing momentum, which differ by the impulse Δp , the functions \mathcal{A} , \mathcal{B} and \mathcal{C} are independent of the specifics of the hard scattering process. We extracted these coefficients from the EFT waveform and reproduced the predictions of Ref. [89].

We have also computed the non-universal \mathcal{D} coefficient and found exact agreement with Eq. (9.11) of [50]. This is the first order in the soft-graviton expansion where the second region mentioned above, in which the Fourier integration variable scales as $q_1 \rightarrow \omega q_1$, first contributes. It is also the first order at which the disconnected cut (5.24) contributes crucially to the match with [50]. The necessity of this term for a successful comparison with the MPM waveform was first suggested in [51] as part of a BMS transformation. In Secs. V A and V C we understood its connection to the disconnected cuts of the observable-based formalism if zero-energy gravitons are part of the spectrum. On the other hand, the ϵ/ϵ term in Eq. (5.16) does not contribute to any of the coefficients in Eq. (6.22) up to a time shift.

VII. TRANSFORMING THE KMOC WAVEFORM TO THE BARRED MOMENTUM FRAME

The MPM waveform $W_{\text{MPM}}(\omega, \theta, \phi)$ is computed in a spatial frame anchored on the classical barred momenta (2.3), while the EFT waveform $\mathcal{W}(\omega, \theta, \phi)$ is originally obtained in a spatial frame anchored on the incoming momenta. Both spatial frames are of the c.m. type, with a negligible $O(G^3)$ difference (due to the radiated momentum) between their time-axes, namely

$$\bar{e}_0^\mu = e_0^\mu + O(G^3). \quad (7.1)$$

At order G^2 the only significant difference between the barred c.m. frame spanned by $(\bar{e}_0, e_x, e_y, e_z)$ (defined in Sec. II) and the frame (e_0, e_1, e_2, e_3) is a spatial rotation of $\chi/2$ mapping the unit vectors e_1, e_2 into e_x, e_y . [Note that in both frames we use a polarization vector respectively anchored on e_1, e_2 or e_x, e_y , as per Eqs. (2.7) and (6.9)].

Consequently, the function of θ and ϕ describing the EFT waveform referred to the barred momenta frame, say $W_{\text{EFT}}(\omega, \theta, \phi)$, is related to the function of θ and ϕ describing the (original) EFT waveform $\mathcal{W}(\omega, \theta, \phi)$ referred to the incoming momenta frame by

$$W_{\text{EFT}}(\omega, \theta, \phi) = \mathcal{W}(\omega, \theta, \phi) + \frac{\chi_{1\text{PM}}}{2} \frac{\partial}{\partial \phi} \mathcal{W}^{G^1}(\omega, \theta, \phi) + O(G^3). \quad (7.2)$$

Here, as indicated, it is sufficient to insert the 1PM [$O(G^1)$] approximation to the scattering angle, namely

$$\chi_{1\text{PM}} = \frac{2G}{b} \frac{2y^2 - 1}{y^2 - 1}. \quad (7.3)$$

Thus, using Eq. (7.2), the comparison between the MPM and EFT waveform is reduced to comparing the function $W_{\text{MPM}}(\omega, \theta, \phi)$ to the function $W_{\text{EFT}}(\omega, \theta, \phi)$.

VIII. COMPARISON BETWEEN MPM AND KMOC WAVEFORMS

When working in the barred momenta frame, the comparison between the MPM waveform and the EFT one amounts to comparing the following two functions of ω, θ, ϕ (and of the impact parameter b): $W^{\text{MPM}}(\omega, \theta, \phi)$ on the one hand, and $W_{\text{EFT}}(\omega, \theta, \phi)$ on the other hand. A complete physical agreement between these two waveforms would mean that these two functions differ at most by the effect of an angular-independent time shift δt . As discussed above, when adding to the EFT waveform the (linearized gravity) contribution coming from the disconnected, zero-frequency diagrams displayed on the left of Fig. 1, the $O(G^0)$ static background (Coulomb-like) contributions in the two waveforms agree with each other [compare Eq. (2.14) with Eq. (5.3)]. In the following, we

¹⁷ This PM calculation was carried out independently in Ref. [51] and both results were presented for the first time at [83, 88]. The calculation was done to 2.5 PN order in Ref. [50].

¹⁸ Note that, while analogous in spirit, is a distinct from the method of regions used to isolate the classical contribution of loop integrals, which have already been evaluated here.

therefore focus on the frequency-dependent parts ($\omega \neq 0$) of the two waveforms, which both start at order G^1 .

Summarizing the results so far, the function $W_{\text{EFT}}(\omega, \theta, \phi)$ can be written (at the one loop accuracy) as the sum of six contributions, namely

$$\begin{aligned} W_{\text{EFT}}(\omega, \theta, \phi) &= \mathcal{W}^{G^1}(\omega, \theta, \phi) + \mathcal{W}^{\text{1 loop } (0)}(\omega, \theta, \phi) \\ &+ \mathcal{W}^{\text{1 loop } \epsilon/\epsilon}(\omega, \theta, \phi) + \mathcal{W}^{\text{1 loop cut}}(\omega, \theta, \phi) \\ &+ \mathcal{W}^{\text{1 loop disc}}(\omega, \theta, \phi) + \delta^{\text{rot}}\mathcal{W}(\omega, \theta, \phi) \\ &+ O(G^3). \end{aligned} \quad (8.1)$$

Here, each term is defined as follows.

The $O(G)$ waveform \mathcal{W}^{G^1} comes from the tree-level matrix element $\mathcal{M}^{\text{tree}}$ in Eq. (5.5),

$$\mathcal{W}^{G^1}(\omega, \theta, \phi) = \frac{2i}{\kappa} \text{FT}_b \left[\mathcal{M}^{\text{tree}} \right]. \quad (8.2)$$

The $O(G^2)$ (one-loop) contributions to the EFT waveform indicated in Eq. (8.1) denote, respectively:

(i) the contribution from the (linear in T) 5-point amplitude obtained by dropping the IR $\frac{1}{\epsilon}$ divergent terms in the results of Refs. [39–41], as displayed in Eq. (5.6) of [50], namely, in the notation introduced in Eq. (8.1) above:

$$\mathcal{W}^{\text{1 loop}(0)} = \frac{2i}{\kappa} \text{FT}_b \left[\kappa^5 m_1^3 m_2^2 \widetilde{\mathcal{M}}_1^{(1)} + (1 \leftrightarrow 2) \right]; \quad (8.3)$$

(ii) the extra, $\frac{\epsilon}{\epsilon}$ contribution from the (linear in T) 5-point amplitude generated after absorbing the IR $\frac{1}{\epsilon}$ divergence into a time shift as discussed in Secs. IV C and V B, namely, in the notation introduced in Eq. (8.1) above:

$$\begin{aligned} \mathcal{W}^{\text{1 loop } \epsilon/\epsilon} &= \frac{2i}{\kappa} \text{FT}_b \left[\kappa^5 m_1^3 m_2^2 \frac{iw_1}{32\pi} \mathcal{M}_{\text{extra}}^{(0)} + (1 \leftrightarrow 2) \right] \\ &= \frac{-2\kappa^4}{32\pi} m_1^2 m_2^2 E \omega \text{FT}_b \left[\mathcal{M}_{\text{extra}}^{(0)} \right]; \end{aligned} \quad (8.4)$$

(iii) the oneloop cut contribution from connected T elements discussed in Sec. V B, namely, in the notation introduced in Eq. (8.1) above:

$$\mathcal{W}^{\text{1 loop cut}} = \frac{2i}{\kappa} \text{FT}_b \left[\mathcal{S}^{\text{1 loop fin}} \right]; \quad (8.5)$$

(iv) the oneloop cut contribution involving disconnected T elements discussed in Sec. V C, namely, in the notation introduced in Eq. (8.1) above:

$$\mathcal{W}^{\text{1 loop disc}} = \frac{2i}{\kappa} \text{FT}_b \left[\mathcal{S}^{\text{1 loop disc}} \right]; \quad (8.6)$$

and finally, (v) the contribution from the spatial rotation between the barred- p frame and the incoming p one discussed in Sec. VII, namely, in the notation introduced in Eq. (8.1) above:

$$\delta^{\text{rot}}\mathcal{W} = +\frac{\chi_{1\text{PM}}}{2} \frac{\partial}{\partial \phi} \mathcal{W}^{G^1}(\omega, \theta, \phi). \quad (8.7)$$

Ref. [50] computed, at the $G^2\eta^5$ accuracy, the (even in ϕ sector of the) difference

$$\delta^{\text{old}}W(\omega, \theta, \phi) \equiv W^{\text{EFT}'}(\omega, \theta, \phi) - W^{\text{MPM}}(\omega, \theta, \phi), \quad (8.8)$$

between the EFT waveform, as it was understood in the first versions of Refs. [39–41], and interpreted in the barred p frame, and the MPM one. In the notation of the present work, the quantity $W^{\text{EFT}'}(\omega, \theta, \phi)$ considered in [50] is equal to

$$W^{\text{EFT}'}(\omega, \theta, \phi) = \mathcal{W}^{G^1}(\omega, \theta, \phi) + \mathcal{W}^{\text{1 loop}(0)}(\omega, \theta, \phi). \quad (8.9)$$

The result of [50] for the difference $\delta^{\text{old}}W(\omega, \theta, \phi)$, Eq. (8.8), was that it started at the G^2/c^5 (2.5PN) level, and contained (at this order) both terms linear in the symmetric mass ratio, ν , and terms quadratic in ν . The explicit expression for the difference

$$\delta^{\text{old}}W(\omega, \theta, \phi) = \delta^\nu W(\omega, \theta, \phi) + \delta^{\nu^2} W(\omega, \theta, \phi) \quad (8.10)$$

was provided in [50] in tensorial form, and in the time domain. See Eqs. (8.10)–(8.13) there. The equivalent result in SWSH form, and in the frequency domain, contains only $l = 2^+$ contributions at order ν^1 , and both $l = 2^+$, $l = 3^-$ and $l = 4^+$ contributions at order ν^2 . Namely,

$$\delta^\nu W(\omega, \theta, \phi) = \sum_{m=2,0,-2} \delta^\nu U_{2m} \bar{Y}_{lm}(\theta, \phi), \quad (8.11)$$

$$\begin{aligned} \delta^{\nu^2} W(\omega, \theta, \phi) &= \sum_{m=2,0,-2} \delta^{\nu^2} U_{2m} \bar{Y}_{2m}(\theta, \phi) \\ &+ \sum_{m=1,-1} \delta^{\nu^2} V_{3m} \bar{Y}_{3m}(\theta, \phi) \\ &+ \sum_{m=4,2,0,-2,-4} \delta^{\nu^2} U_{4m} \bar{Y}_{4m}(\theta, \phi), \end{aligned} \quad (8.12)$$

with

$$\begin{aligned} \delta^\nu U_{22} &= -\frac{4i\sqrt{5\pi}}{5} \frac{G^2 M^3}{b} p_\infty^2 \nu u [K_0(u) - 2K_1(u)], \\ \delta^\nu U_{20} &= -\frac{4i\sqrt{30\pi}}{15} \frac{G^2 M^3}{b} p_\infty^2 \nu u [K_0(u) + 2uK_1(u)], \\ \delta^\nu U_{22} &= -\frac{4i\sqrt{5\pi}}{5} \frac{G^2 M^3}{b} p_\infty^2 \nu u [K_0(u) + 2K_1(u)], \end{aligned} \quad (8.13)$$

$$\begin{aligned} \delta^{\nu^2} U_{22} &= \frac{8i\sqrt{5\pi}}{105} \frac{G^2 M^3}{b} p_\infty^2 \nu^2 u [(13u + 6)K_0(u) \\ &+ 13(u + 1)K_1(u)], \\ \delta^{\nu^2} U_{20} &= \frac{8i\sqrt{30\pi}}{105} \frac{G^2 M^3}{b} p_\infty^2 \nu^2 u [2K_0(u) - uK_1(u)], \\ \delta^{\nu^2} U_{22} &= \frac{8i\sqrt{5\pi}}{105} \frac{G^2 M^3}{b} p_\infty^2 \nu^2 u [(-13u + 6)K_0(u) \\ &+ 13(u - 1)K_1(u)], \end{aligned} \quad (8.14)$$

$$\begin{aligned}
\delta^{\nu^2} V_{32} &= -\frac{2i\sqrt{7\pi}}{21} \frac{G^2 M^3}{b} p_\infty^2 \nu^2 u [u K_0(u) \\
&\quad + (1+u) K_1(u)], \\
\delta^{\nu^2} V_{30} &= -\frac{2i\sqrt{210\pi}}{105} \frac{G^2 M^3}{b} p_\infty^2 \nu^2 u [u K_0(u) + K_1(u)], \\
\delta^{\nu^2} V_{3\bar{2}} &= -\frac{2i\sqrt{7\pi}}{21} \frac{G^2 M^3}{b} p_\infty^2 \nu^2 u [u K_0(u) \\
&\quad + (1-u) K_1(u)], \tag{8.15}
\end{aligned}$$

$$\begin{aligned}
\delta^{\nu^2} U_{44} &= -\frac{i\sqrt{7\pi}}{21} \frac{G^2 M^3}{b} p_\infty^2 \nu^2 u [(1+2u) K_0(u) \\
&\quad + 2(u+1) K_1(u)], \\
\delta^{\nu^2} U_{42} &= -\frac{2i\sqrt{\pi}}{21} \frac{G^2 M^3}{b} p_\infty^2 \nu^2 u (u+1) [K_0(u) + K_1(u)], \\
\delta^{\nu^2} U_{40} &= -\frac{i\sqrt{10\pi}}{105} \frac{G^2 M^3}{b} p_\infty^2 \nu^2 u [3K_0(u) + 2u K_1(u)], \\
\delta^{\nu^2} U_{4\bar{2}} &= -\frac{2i\sqrt{\pi}}{21} \frac{G^2 M^3}{b} p_\infty^2 \nu^2 u (1-u) [K_0(u) - K_1(u)], \\
\delta^{\nu^2} U_{4\bar{4}} &= -\frac{i\sqrt{7\pi}}{21} \frac{G^2 M^3}{b} p_\infty^2 \nu^2 u [(1-2u) K_0(u) \\
&\quad + 2(u-1) K_1(u)]. \tag{8.16}
\end{aligned}$$

Note that, $W^{\text{EFT}'}$ did not (on purpose¹⁹) contain the $\frac{\chi}{2}$ rotation contribution, $\delta^{\text{rot}}\mathcal{W}$, nor the three new contributions discussed in the present work, namely $\mathcal{W}^{\text{1 loop } \epsilon/\epsilon}$, $\mathcal{W}^{\text{1 loop cut}}$ and $\mathcal{W}^{\text{1 loop disc}}$. Therefore, updating the comparison done in [50] leads to a new difference

$$\delta^{\text{new}} W(\omega, \theta, \phi) \equiv W^{\text{EFT}}(\omega, \theta, \phi) - W^{\text{MPM}}(\omega, \theta, \phi), \tag{8.17}$$

given by

$$\begin{aligned}
\delta^{\text{new}} W &= \delta^{\text{old}} W + \mathcal{W}^{\text{1 loop } \epsilon/\epsilon} + \mathcal{W}^{\text{1 loop cut}} \\
&\quad + \mathcal{W}^{\text{1 loop disc}} + \delta^{\text{rot}}\mathcal{W}. \tag{8.18}
\end{aligned}$$

As we shall discuss next, the additional contributions (new with this work) displayed in Eq. (8.18) are such that they precisely cancel the two types ($O(\nu^1)$ and $O(\nu^2)$) of discrepancies that were present in Eq. (8.8), modulo an angular-independent time-shift between the two waveforms.

IX. KMOC CUT AND FRAME ROTATION

It was first noticed in [50] by directly comparing the MPM waveform with the amplitude contribution to the KMOC waveform that, up to 2PN order, there is a remarkable agreement between the two when the latter is

¹⁹Indeed, one of the important findings of [50] was the need to rotate the EFT to the barred p frame, otherwise the MPM/EFT mismatch would start at the Newtonian order, instead of being relegated to the 2.5PN order.

evaluated in the frame rotated by half the scattering angle relative to the incoming frame (i.e. in the barred frame). As mentioned earlier, this raised the possibility that the cut contribution could be absorbed into this frame change, which is further confirmed in the soft graviton expansion discussed in Sec. VI C.

By Fourier-transforming the one-loop *connected* cut contribution to impact-parameter space, Ref. [51] showed that $\mathcal{W}^{\text{1 loop cut}}$ can be written as a certain differential operator acting on the tree-level waveform up to a further finite redefinition of the retarded time. In the coordinates used here this differential operator acts as a rotation by $\chi/2$. Using the explicit expression of the connected cut [39, 41, 91], we explicitly verified this relation,

$$\mathcal{W}^{\text{1 loop cut}} = -\frac{\chi_{1\text{PM}}}{2} \frac{\partial}{\partial \phi} \mathcal{W}^{\text{tree}} + i\omega \delta t^{\text{cut}} \mathcal{W}^{\text{tree}}, \tag{9.1}$$

up to 3PN order. The ϵ/ϵ term in the second Eq. (5.16) plays a crucial role.²⁰ Resumming the 3PN-accurate expansion of the time shift (which starts at Newtonian order) yields the following all-order-in- p_∞ expression

$$\begin{aligned}
\delta t^{\text{cut}} &= \frac{\kappa^2 E}{32\pi} \left[\Gamma \log \frac{\mu_{\text{IR}} b e^{\gamma_E}}{2} - \frac{y}{2(y^2 - 1)^{3/2}} \right. \\
&\quad \left. + \frac{E_1 E_2 (2y^2 - 1)}{m_1 m_2 (y^2 - 1)^{3/2}} \right]. \tag{9.2}
\end{aligned}$$

To compare with Eq. (3.48) of the version 1 of Ref. [51], we include the IR-divergent term in Eq. (5.12) to the left hand side (to obtain $\text{FT}_b[\mathcal{S}^{\text{1 loop}}]$) and the time shift $\delta t_{\text{IR}}^{\text{cut}} = -\frac{GE\Gamma}{2\epsilon}$ that cancels it to the right hand side. This gives,

$$\begin{aligned}
\text{FT}_b[\mathcal{S}^{\text{1 loop}}] &= -\frac{\chi_{1\text{PM}}}{2} \frac{\partial}{\partial \phi} \text{FT}_b[\mathcal{M}^{\text{tree}}] \\
&\quad + i\omega \delta T^{\text{cut}} \text{FT}_b[\mathcal{M}^{\text{tree}}], \tag{9.3}
\end{aligned}$$

where $\delta T^{\text{cut}} = \delta t^{\text{cut}} + \delta t_{\text{IR}}^{\text{cut}}$. Through $O(\epsilon^0)$ our time shift agrees with the result of the version 1 of Ref. [51]

$$\begin{aligned}
\delta T^{\text{cut}} &= \frac{\kappa^2 E}{32\pi} \left[\frac{y(y^2 - \frac{3-4\epsilon}{2-2\epsilon})}{(y^2 - 1)^{3/2}} \frac{e^{\epsilon\gamma_E} \Gamma(-\epsilon)}{(\mu_{\text{IR}}^2 b^2/4)^{-\epsilon}} \right. \\
&\quad \left. + \frac{E_1 E_2 (2y^2 - 1)}{m_1 m_2 (y^2 - 1)^{3/2}} \right]. \tag{9.4}
\end{aligned}$$

Together with the observation that in our c.m. frame the operator $\bar{\delta}$ in [51] becomes $-(\chi_{1\text{PM}}/2)\partial_\phi$, we find exact agreement with the prediction of Ref. [51] (up to a redefinition of the arbitrary scale μ_{IR}), which we have thus verified through direct evaluation up to $O(p_\infty^3)$, or 3PN order.

²⁰As our results were written up, we became aware that this point was also explicitly noted in the version 2 update of Ref. [51].

In light of this agreement, let us comment on the technical differences between the setup discussed here and that of Ref. [51]. Certain steps in our evaluation and simplification of the cut term, such as removal of terms proportional to the Gram determinant of five vectors, assumed that the external kinematics, including the momentum transfer, were four-dimensional. Consequently, all our Fourier transforms were strictly in four dimensions, as enforced by the decomposition of the momentum transfer in Eq. (6.12). In contrast, the setup in Ref. [51] assumes that the Fourier transform is d -dimensional. Interestingly, this does not appear to have any consequences in the comparison, such as a difference in the ϵ/ϵ contributions that build on the IR-divergent terms.

The analysis outlined in this section indicates that when comparing the EFT and MPM result in the barred c.m. frame, we can effectively ignore the connected cut contribution $\mathcal{S}^1 \text{loop}$ altogether, as it is cancelled by the frame rotation up to a time shift. In other words, we can rewrite Eq. (8.18) in the simplified form

$$\begin{aligned} \delta^{\text{new}} W &= \delta^{\text{old}} W + \mathcal{W}^1 \text{loop } \epsilon/\epsilon + \\ &+ \mathcal{W}^1 \text{loop disc} + \text{time shift} . \end{aligned} \quad (9.5)$$

We now proceed to discuss the remaining two terms, $\mathcal{W}^1 \text{loop } \epsilon/\epsilon$ and $\mathcal{W}^1 \text{loop disc}$.

X. $\mathcal{W}^1 \text{loop } \epsilon/\epsilon$ AND $\delta^\nu W$

The additional ϵ/ϵ contribution is given by Eq. (8.4). Remembering the presence of a factor $1/(m_1 m_2)$ in the Jacobian of FT_b , $\mathcal{W}^1 \text{loop } \epsilon/\epsilon$ is seen to be proportional to $m_1 m_2$, i.e. to be proportional to ν^1 . In addition, as it contains a $O(\eta^3)$ factor $GE\omega = \frac{GM\omega}{c^3}$, and as $\mathcal{M}_{\text{extra}}^{(0)}$ is easily seen to start to differ from its full-gravity tree-level counterpart $\mathcal{M}_{d=4}^{(0)}$ only at the 1PN, $O(\eta^2)$, level, we conclude that $\mathcal{W}^1 \text{loop } \epsilon/\epsilon$ effectively (i.e. modulo a time shift) starts contributing to W at the $G^2\eta^5$ level.

An easy computation of the impact-parameter transform of the PN expansion of $\mathcal{M}_{\text{extra}}^{(0)}$ actually shows that, modulo a time-shift contribution, $i\omega\delta t W^{G^1}$, the even-in- ϕ projection of $\mathcal{W}^1 \text{loop } \epsilon/\epsilon$ precisely cancels the $O(\nu)$, $G^2\eta^5$ -level, contribution $\delta^\nu W(\omega, \theta, \phi)$ found (in [50]) to be present in $\delta W(\omega, \theta, \phi)$, and displayed in Eq. (8.13). Namely,

$$\delta^\nu W + \left[\mathcal{W}^1 \text{loop } \epsilon/\epsilon + i\omega\delta t^{\epsilon/\epsilon} W^{G^1} \right]^{\phi-\text{even}} = O\left(\frac{G^2}{c^6}\right), \quad (10.1)$$

with $\delta t^{\epsilon/\epsilon} = \frac{GE}{c^5} = \frac{GM}{c^3}(1 + \frac{\nu}{2}p_\infty^2 + O(p_\infty^4))$.

XI. $\mathcal{W}^1 \text{loop disc}$ AND $\delta^{\nu^2} W$

The final terms to discuss (at the highest PN accuracy explicitly studied in [50]) are the (even-in- ϕ projection of the) disconnected cut contribution to \mathcal{W} and the

$O(\nu^2)$, $G^2\eta^5$ -level, contribution $\delta^{\nu^2} W(\omega, \theta, \phi)$ displayed in Eqs. (8.14), (8.15) and (8.16).

It was suggested in Ref. [51] that the difference $\delta^{\nu^2} W(\omega, \theta, \phi)$ is genuinely present in the EFT-MPM difference and corresponds to the fact that the EFT waveform does not contain some of the zero-frequency-graviton effects contained in the MPM waveform, because it works in the canonical BMS frame of [52] (in which $W(t = -\infty) = 0$) rather than in the intrinsic BMS frame selected both by standard classical PM theory and the MPM formalism. However, we found in Sec. V that disconnected contributions to the cut term account for this. They lead to the additional term $\mathcal{W}^1 \text{loop disc}$ in the EFT waveform whose explicit form is

$$\mathcal{W}^1 \text{loop disc} = +iG \left[m_1 w_1 \log \frac{w_1^2}{\omega^2} + m_2 w_2 \log \frac{w_2^2}{\omega^2} \right] \mathcal{W}^{G^1}. \quad (11.1)$$

This term is $O(\nu^2)$, and its PN expansion starts at the G^2/c^5 level. An easy computation shows that its ϕ -even projection exactly cancels, at this order, all the $l = 2^+, l = 3^-$ and $l = 4^+$ pieces of $\delta^{\nu^2} W(\omega, \theta, \phi)$ displayed in Eqs. (8.14), (8.15) and (8.16):

$$\delta^{\nu^2} W + [\mathcal{W}^1 \text{loop disc}]^{\phi-\text{even}} = O\left(\frac{G^2}{c^6}\right), \quad (11.2)$$

without the need of an additional time-shift.

In other words, after factoring out the effect of the $\chi/2$ rotation, the total time-shift needed to align the MPM waveform (defined as in [50]) and the EFT one (completed by the ϵ/ϵ and the disconnected contributions) is $\delta t^{\text{tot}} = GM/c^3$. This time-shift can be absorbed in a modification of the link between the time scale b_0 entering the tail logarithms of the MPM formalism and the frequency scale μ_{IR} of the amplitudes-based formalism. Namely, Eq. (8.8) of [50] is modified into

$$\log(2b_0\mu_{\text{IR}}) + \gamma_E = 0. \quad (11.3)$$

Note the curious feature that the additional term, Eq. (11.1), which reads,

$$\mathcal{W}^1 \text{loop disc} = i\omega\delta t^{\text{VV}}(\theta, \phi)W^{G^1}, \quad (11.4)$$

with the angle-dependent time shift

$$\delta t^{\text{VV}}(\theta, \phi) = 2G \left(m_1 \frac{w_1}{\omega} \log \frac{w_1}{\omega} + m_2 \frac{w_2}{\omega} \log \frac{w_2}{\omega} \right), \quad (11.5)$$

doubles, rather than cancels, the contribution to the EFT waveform coming from the last two lines in Eq. (5.22) of Ref. [50]. See further discussion of this term below.

The results (9.3), (10.1) and (11.2) allow us to conclude that the inclusion of the new contributions discussed in this work to the EFT waveform resolves all the mismatches with the even-in- ϕ projection of the $G^2\eta^5$ -accurate MPM waveform computed in [50].

To complete the EFT-MPM comparison on the odd-in- ϕ sector, we have also compared the odd-in- ϕ projection

of W^{MPM} , at the $G^2(\eta^1 + \eta^4)$ accuracy (see Eqs. (3.25) and (3.27)) with its EFT counterpart (given, in the equatorial plane, in the ancillary file `PNexpandedEFT.nb`). We found perfect agreement between the two (with the same time-shift needed for the ϕ -even part, i.e. the same link Eq. (11.3)). Though our checks in the odd-in- ϕ sector probe nonlinear contributions to the waveform less deeply than our even-in- ϕ checks, they still include the leading-order tail contributions, and are sensitive to the precise relation Eq. (11.3). The explicit comparison between the MPM and amplitudes-based waveforms is presented in the ancillary file `MPMEFTcomparison.nb`.

XII. CONCLUSIONS

We revisited the amplitude- and observable-based (KMOC [3]) derivation of the classical gravitational wave signal emitted during the scattering of two non-spinning masses at the NNLO order $h_{\mu\nu} = g_{\mu\nu} - \eta_{\mu\nu} \sim G^1 + G^2 + G^3$, and compared our results for the frequency-domain, G -rescaled waveform quantity $W(\omega, \theta, \phi) \equiv \frac{c^4}{4G} \varepsilon^\mu \varepsilon^\nu h_{\mu\nu} \sim G^0 + G^1 + G^2$, to the corresponding waveform derived within the (post-Newtonian-matched) Multipolar-post-Minkowskian (MPM) formalism. The recent computation of $W^{\text{MPM}}(\omega, \theta, \phi)$ [50] had pointed out the presence of large discrepancies (starting at the Newtonian level) between $W^{\text{MPM}}(\omega, \theta, \phi)$ and the (finite part of the) amplitude-based waveform derived in the (first versions of) Refs. [39–41], say $W^{\text{EFT}'}(\omega, \theta, \phi)$. Ref. [50] had further pointed out that the EFT/MPM mismatch was drastically reduced from the Newtonian level $G^2\eta^0$ (where $\eta \equiv \frac{1}{c}$) to the 2.5 PN level $G^2\eta^5$ by rotating (by half the classical scattering angle $\chi/2$) the EFT waveform from the incoming momenta frame to the (classical) averaged momenta frame. Part of the puzzle posed by the EFT/MPM mismatch was recently clarified by the eikonal-inspired approach of Georgoudis, Heissenberg and Russo [51] who argued that the cut contribution needed [42] in the KMOC framework (and missing in the first derivations of the EFT waveform) was precisely implementing the needed rotation between the incoming-momenta frame (naturally tuned to $W^{\text{EFT}}(\omega, \theta, \phi)$) and the (classical) averaged-momenta frame (conveniently used to compute $W^{\text{MPM}}(\omega, \theta, \phi)$) for all final-states that do not contain zero-energy gravitons. Ref. [51] compared only the soft expansion of $W^{\text{EFT}}(\omega, \theta, \phi)$ to the soft expansion of $W^{\text{MPM}}(\omega, \theta, \phi)$ and could indeed verify that the $\chi/2$ rotational effect of the cut term reduced the EFT/MPM mismatch between these expansions to the $G^2\eta^5$ level. However, the soft limit is a rather blunt tool which is not sensitive to the details of the EFT/MPM mismatch (as discussed, e.g., in Section IX of [50]).

Indeed, after factoring out the effect of the $\chi/2$ rotation, the EFT-MPM mismatch found in [50] still contained significant terms of order $\nu^1 G^2 \eta^5$ and of order $\nu^2 G^2 \eta^5$. The terms $O(\nu^1 G^2 \eta^5)$ effectively disappear in

the soft limit (because they are equivalent to an unobservable time shift). We showed in the present work that a subtle additional ϵ/ϵ contribution to the amplitude result (coming, in our scheme, from the tracelessness of the physical graviton in d dimensions) precisely cancelled the $O(\nu^1 G^2 \eta^5)$ EFT-MPM mismatch (which could not be seen in the soft limit). Concerning the last remaining $O(\nu^2 G^2 \eta^5)$ EFT-MPM mismatch, it was argued by Georgoudis et al. [51] that it remained and that, in view of Eqs. (11.1), (11.5), it was to be physically interpreted as the presence of the particular $O(G)$ supertranslation (i.e. an angle-dependent time shift) $\delta t^{\text{VV}}(\theta, \phi)$, Eq. (11.5), pointed out by Veneziano and Vilkovisky [52], for its role in transforming the “intrinsic” BMS frame (naturally used both in classical, worldline PM perturbation theory, and in the MPM formalism) into the “canonical” BMS frame (defined so that the initial value of the waveform vanishes in the infinite past). The interpretation of the necessary presence of the supertranslation (11.5) was that this supertranslation removes the effect of static modes (zero-frequency gravitons) in the waveform, and that the amplitude approach naturally computes a waveform without static modes. Our new results suggest, however, a different picture. Static modes can be incorporated in the KMOC waveform if one includes disconnected T -matrix elements, both at the linear-in- T level and at the bilinear-in- T level (cut term). We have explicitly shown (see Eq. (5.3)) that the inclusion of disconnected diagrams (pictured in Fig. 1a) to the linear-in- T waveform was precisely generating the initial, zero-frequency contribution which is naturally present in the MPM waveform (see Eq. (2.13)). The situation concerning the effect of disconnected diagrams in the bilinear-in- T term is more subtle. In a natural regularization which takes the matter velocity slightly off-shell, $u_3 \rightarrow \tilde{u}_3$, we showed both by direct evaluation and by interpreting it as the discontinuity of a triangle integral that the cut pictured in Fig. 1b yields an additional contribution to W_{EFT} that precisely cancels the effect of the supertranslation (11.5), thereby removing the last remaining $O(\nu^2 G^2 \eta^5)$ EFT-MPM mismatch. We have also shown in App. D that higher-loop contributions would not modify our finding. It would clearly be interesting to confirm in a different way our conclusion that the inclusion of disconnected diagrams in the KMOC formalism does incorporate all the physical effects linked to the static modes (which are included in the MPM formalism). It would also be interesting to know whether a higher-order KMOC calculation, systematically ignoring disconnected diagrams, would automatically yield a waveform differing from the MPM one *only* by taking into account the full (nonlinear) effect of the supertranslation (11.5) (which is fully determined by the $O(G)$ linearized-gravity Coulombic background (2.13), (2.14)). A classical (worldline-based) PM-gravity computation (à la [9, 92, 93]) of the one-loop waveform would be very valuable. Conversely, it would be interesting to explore if the time-dependent and time-independent contributions of zero-energy gravitons

tons can be captured by a nontrivial vacuum containing a coherent state or condensate of such modes, perhaps along the lines of [78, 85, 94].

In this paper we have shown the agreement between the MPM and EFT waveforms (over the full celestial sphere) at the $(G+G^2)(\eta^0+\eta^2+\eta^3+\eta^5)$ accuracy (2.5PN order) in the ϕ -even sector, and at the $(G+G^2)(\eta^1+\eta^4)$ accuracy in the ϕ -odd sector. [The agreement of the ϕ -even $(G+G^2)\eta^4$ (2PN) terms was also separately checked in the equatorial plane.] The details of our results are presented in three ancillary files: (1) the PN expansions of the spin-weighted-spherical-harmonic coefficients W_{lm}^{MPM} of the MPM waveform $W^{\text{MPM}}(\theta, \phi)$ are given in the ancillary file `MPMmultipoles.nb` so as to reach the accuracy $(G+G^2)(\eta^0+\eta^2+\eta^3+\eta^4+\eta^5)$ for even m 's (ϕ -even sector; which has been extended here to include the 2PN terms) and the accuracy $(G+G^2)(\eta^1+\eta^4)$ for odd m 's (ϕ -odd sector); (2) the PN-expansion of the $\theta = \frac{\pi}{2}$ restriction of the rotated one-loop-accurate EFT waveform $W_{\text{EFT}}(\omega, \theta, \phi)$, Eq. (7.2), is given in the ancillary file `PNexpandedEFT.nb` at the 3PN accuracy, i.e. $(G+G^2)(\eta^0+\eta^1+\eta^2+\eta^3+\eta^4+\eta^5+\eta^6)$; and (3) the comparison (and agreement), in the equatorial plane, between the two waveforms is presented in the ancillary file `MPMEFTcomparison.nb`.

Our current organization of the amplitude and cut contributions, in terms of functions free of spurious poles, makes it possible to proceed to higher PN orders at $O(G^3)$ in the EFT side. By contrast, analogous extensions on the MPM side require (when using the MPM techniques used so far) to compute new, challenging, higher-PN contributions. This suggests that borrowing information from the EFT calculation might help to improve the power of the MPM formalism. Moreover, it would undoubtedly be interesting to extend our comparison to scattering waveforms for spinning bodies, for which the MPM formalism naturally applies [7, 95] and $O(G^3)$ amplitudes-based results are available [46].

The $O(G^3)$ waveform discussed here allows for a direct determination of the $O(G^4)$ angular momentum and energy loss which have nontrivial implications for conservative binary scattering at $O(G^5)$, including information on the first second-self-force contribution to this process. Carrying out the next-order waveform calculation, which both gives analogous information $O(G^6)$ and probes the agreement between EFT and MPM at higher orders in Newton's constant, poses an interesting and important challenge to the EFT calculation, through the more involved multi-scale integration-by-parts reduction and the evaluation of the ensuing multi-scale master integrals and of the Fourier-transform to impact parameter space.

One of the important takeaway messages of our new results is that, after having sorted out the subtleties that were hidden in the EFT one-loop waveform, we obtained a remarkable confirmation that the classical limit of an amplitude-based waveform does correctly incorporate the many subtle classical effects that were included in the $O(G^2\eta^5)$ -accurate MPM waveform such

as (i) radiation-reaction effects on the worldlines, (ii) high-multipolarity tail effects in the wave-zone, and (iii) cubically nonlinear multipole couplings in the exterior zone. The fact that the road leading to the present successful EFT/MPM comparison had some bumps, which taught us interesting lessons, is another example of the useful synergy between amplitude-based, and classical perturbation-theory-based, approaches to gravitational physics.

ACKNOWLEDGMENTS

We thank Holmfridur Hannesdottir, Sebastian Mizera, and Cristian Vergu for discussions; RR and FT thank Enrico Herrmann and Michael Ruf for emphasizing the importance of zero-energy modes. We also thank Alessandro Georgoudis, Carlo Heissenberg and Rodolfo Russo for discussions and communications on the submission. The present research was partially supported by the 2021 Balzan Prize for Gravitation: Physical and Astrophysical Aspects, awarded to T. Damour. D.B. acknowledges the sponsorship of the Italian Gruppo Nazionale per la Fisica Matematica (GNFM) of the Istituto Nazionale di Alta Matematica (INDAM), as well as the hospitality and the highly stimulating environment of the Institut des Hautes Etudes Scientifiques. S.D.A.'s research is supported by the European Research Council, under grant ERC-AdG-88541. A.H. is supported by the Simons Foundation. R.R. and F.T. are supported by the U.S. Department of Energy (DOE) under award number DE-SC00019066.

Appendix A: Notations

In this appendix, we collect the various notations used in the main text:

$$\begin{aligned}
\kappa^2 &= 32\pi G \\
\eta_{\mu\nu} &= \text{diag}(-1, +1, +1, +1) \\
g_{\mu\nu} &= \eta_{\mu\nu} + h_{\mu\nu} = \eta_{\mu\nu} + \kappa h_{\mu\nu} \\
w_1 &= -u_1 \cdot k \quad w_2 = -u_2 \cdot k \\
y &= -u_1 \cdot u_2 \quad \Gamma = \frac{3y - 2y^3}{(y^2 - 1)^{3/2}} \\
F_{\mu\nu} &= k_\mu \varepsilon_\nu - k_\nu \varepsilon_\mu \\
F_1 &= F_{\mu\nu} q_1^\mu u_1^\nu \\
F_2 &= F_{\mu\nu} q_2^\mu u_2^\nu \\
F_3 &= F_{\mu\nu} u_1^\mu u_2^\nu \\
E &= \sqrt{m_1^2 + 2ym_1m_2 + m_2^2} \\
E_1 &= \frac{m_1}{E}(ym_2 + m_1) \quad E_2 = \frac{m_2}{E}(ym_1 + m_2) \\
P_{\text{c.m.}} &= \frac{m_1 m_2}{E} \sqrt{y^2 - 1} \\
p_\infty &= \sqrt{y^2 - 1}
\end{aligned}$$

$$\begin{aligned} M &= m_1 + m_2 & \nu &= \frac{m_1 m_2}{(m_1 + m_2)^2} \\ M &= \frac{E}{c^2} & \eta &= \frac{1}{c} \end{aligned}$$

The speed of light is set to unity, $c = 1$, unless it is useful to emphasize the PN order.

Appendix B: One-loop amplitude and KMOC cut

Here we collect the one-loop amplitude and cut contribution to the KMOC matrix element \mathcal{M} that are known in the literature. We follow the notation used in [41], which was also used in [50]. The IR finite part of the classical one-loop five-point amplitude is given by

$$\begin{aligned} \widetilde{\mathcal{M}}_1^{(1)} = & \left[\frac{i w_1}{32\pi} \log \frac{w_1^2}{\mu_{\text{IR}}^2} + \frac{w_1}{32} + \frac{\Gamma w_1}{64} \right] \mathcal{M}_{d=4}^{(0)} + \frac{\Re}{\pi} + \mathfrak{c}_1 \mathcal{I}_1 \\ & + \mathfrak{c}_2 \mathcal{I}_2 + \frac{\mathfrak{l}_q}{\pi} \log \frac{q_1^2}{q_2^2} + \frac{\mathfrak{l}_{w_2}}{\pi} \log \frac{w_2^2}{w_1^2} + \frac{\mathfrak{l}_y}{\pi} \frac{\text{arccosh} y}{\sqrt{y^2 - 1}}, \end{aligned} \quad (\text{B1})$$

where μ_{IR} is the arbitrary scale introduced by the dimensional regularization, and $\mathcal{I}_{1,2}$ are two triangle integrals,

$$\begin{aligned} \mathcal{I}_1 &= -\frac{i}{32\sqrt{q_2^2 + w_1^2}} + \frac{1}{16\pi\sqrt{q_2^2 + w_1^2}} \text{arcsinh} \frac{-w_1}{\sqrt{q_2^2}}. \\ \mathcal{I}_2 &= -\frac{i}{32\sqrt{q_1^2}}. \end{aligned} \quad (\text{B2})$$

The gauge invariant coefficients \Re , $\mathfrak{c}_{1,2}$ and $\mathfrak{l}_{q,w_2,y}$ are functions of the kinematic data $w_{1,2}$, $q_{1,2}^2$, $F_{1,2,3}$ and y . Their explicit expressions can be found in the ancillary files of [41].

The IR finite part of the one-loop KMOC cut is

$$\begin{aligned} \mathcal{S}_1^{(1)} = & \frac{i w_1 \Gamma}{64\pi} \mathcal{M}_{d=4}^{(0)} \log \mu_{\text{IR}}^2 + \mathfrak{c}_{\text{rat}} + \mathfrak{c}_{q_1} \log q_1^2 \\ & + \mathfrak{c}_{q_2} \log q_2^2 + \mathfrak{c}_{w_1} \log w_1^2 + \mathfrak{c}_{w_2} \log w_2^2 \\ & + \mathfrak{c}_y^{(1)} \frac{\log(y^2 - 1)}{\sqrt{y^2 - 1}} + \mathfrak{c}_y^{(2)} \text{arccosh} y, \end{aligned} \quad (\text{B3})$$

where the \mathfrak{c} -coefficients can also be found in the ancillary files of [41].

Appendix C: Reorganization of the one-loop five-point amplitude free of spurious poles

By direct inspection of the rational coefficients appearing in Eq. (5.11) and App. B (which can be found in the ancillary files of [39, 41, 46]), we find four SPs (which correspond to lower dimensional Gram determinants) in the physical region, plus two additional SPs on the physical sheet (but for complex kinematics). The former four are, respectively, given by the vanishing loci of

$$\begin{aligned} \Delta_1 &\equiv y - \frac{w_1^2 + w_2^2}{2w_1 w_2}, \\ \Delta_2 &\equiv y - \frac{(q_1^2 w_1)^2 + (q_2^2 w_2)^2}{2q_1^2 q_2^2 w_1 w_2}, \\ \Delta_3 &\equiv (q_1^2 - q_2^2)^2 - 4w_1^2 q_1^2, \\ \Delta_4 &\equiv (q_1^2 - q_2^2)^2 - 4w_2^2 q_2^2; \end{aligned} \quad (\text{C1})$$

the latter two are located, respectively, at the zeroes of²¹

$$\begin{aligned} \Pi_1 &\equiv w_1^2 + q_2^2, \\ \Pi_2 &\equiv w_2^2 + q_1^2. \end{aligned} \quad (\text{C2})$$

At $\Delta_{1,2} = 0$, we find second-order poles in the rational coefficients $\mathfrak{l}_{q,w,y}$ and simple poles in \Re . We first focus on Δ_1 and then trivially generalize the result to analogous poles at $\Delta_2 = 0$ through the substitution $w_i \rightarrow w_i q_i^2$, which maps Δ_1 into Δ_2 .

The cancellation of the second-order poles requires that we construct combinations of square roots and logarithms that are proportional to Δ_1^2 . To understand the pattern, we expand $\text{arccosh} y$ around $\Delta_1 = 0$:

$$\begin{aligned} \frac{\text{arccosh} y}{\sqrt{y^2 - 1}} = & \left(\frac{2z}{z^2 - 1} - \frac{4z^2(1+z^2)}{(z^2 - 1)^3} \Delta_1 \right) \log z \\ & + \frac{4z^2}{(z^2 - 1)^2} \Delta_1 + O(\Delta_1^2), \end{aligned} \quad (\text{C3})$$

where $z = \frac{w_2}{w_1}$ and the expansion is symmetric in $z \rightarrow \frac{1}{z}$. This expansion indicates that the following combination of logarithms,

$$\log z - \frac{z^2 - 1}{2z} \left[\left(1 + \frac{y \Delta_1}{y^2 - 1} \right) \frac{\text{arccosh} y}{\sqrt{y^2 - 1}} - \frac{\Delta_1}{y^2 - 1} \right] = O(\Delta_1^2), \quad (\text{C4})$$

²¹ A note of caution should be made about these additional singularities. The sign of the $i\epsilon$ prescription for w_1 determines whether or not the integral \mathcal{I}_1 has a branch point at Π_1 in the complex q_1^2

plane. We use the prescription $w_1 \rightarrow w_1 + i\epsilon$, which does not give a singularity at Π_1 . The SP also cancels among the coefficient of \mathcal{I}_1 and the rational terms \Re .

should lead to expressions that are free of second-order SPs in Δ_1 and Δ_2 . This is indeed the case and we thus found the first two desired functions:

$$L_w = \frac{1}{\Delta_1^2} \left\{ 2 \log \frac{w_2}{w_1} - \frac{w_2^2 - w_1^2}{w_1 w_2} \left[\left(1 + \frac{y \Delta_1}{y^2 - 1} \right) \frac{\operatorname{arccosh} y}{\sqrt{y^2 - 1}} - \frac{\Delta_1}{y^2 - 1} \right] \right\}, \quad (\text{C5})$$

$$L_q = \frac{1}{\Delta_2^2} \left\{ 2 \log \frac{q_2^2}{q_1^2} + 2 \log \frac{w_2}{w_1} - \frac{(q_2^2 w_2)^2 - (q_1^2 w_1)^2}{q_1^2 q_2^2 w_1 w_2} \left[\left(1 + \frac{y \Delta_2}{y^2 - 1} \right) \frac{\operatorname{arccosh} y}{\sqrt{y^2 - 1}} - \frac{\Delta_2}{y^2 - 1} \right] \right\}. \quad (\text{C6})$$

We stress that such functions are not unique since any term $O(\Delta_i^0)$ can be added without changing the desired properties.

We next turn our attention to the poles in Δ_3 and Π_1 , which are closely related and are of fourth and third order, respectively, in the part of the amplitude proportional to $m_1^3 m_2^2$. When constructing an ansatz for SP-free functions we should account for the fact that Π_1 appears only in the coefficient of \mathcal{I}_1 and in \mathfrak{R} and thus we should not include it together with \mathcal{I}_2 and $\log \frac{q_1^2}{q_2^2}$. Further accounting for the order of the pole in Π_1 , a suitable ansatz is

$$\frac{\Delta_3 P_1}{(q_1^2)^4 w_1^5 \Pi_1^3} + \frac{P_2}{(q_1^2)^4 \Pi_1^3} \mathcal{I}_1 + \frac{P_3}{(q_1^2)^4 w_1^4} \log \frac{q_1^2}{q_2^2} + \mathcal{I}_2. \quad (\text{C7})$$

In this expression P_i 's are arbitrary polynomials in q_1^2 , q_2^2 and w_1 ; they are fixed by demanding that this expression has a four-th order zero at $\Delta_3 = 0$ and cubic zero at $\Pi_1 = 0$ (which is away from the physical region). Thus, a function with no SPs in Δ_3 is

$$\begin{aligned} I_1 = & -\frac{q_1^2 + q_2^2}{256\pi(q_1^2)^2 w_1 \Pi_1 \Delta_3} \left(\frac{3(q_2^2)^2 + 11q_2^2 w_1^2 + 23w_1^4}{384(q_1^2 w_1^2)^2 \Pi_1^2} - \frac{q_2^2 + 4w_1^2}{16q_1^2 w_1^2 \Pi_1 \Delta_3} + \frac{1}{\Delta_3^2} \right) \\ & + \frac{q_1^2 + q_2^2}{128(q_1^2)^4 \Pi_1^3 \Delta_3} \left[\frac{35}{16} - \frac{35(q_1^2 + q_2^2)^2}{8\Delta_3} + \frac{7(q_1^2 + q_2^2)^4}{2\Delta_3^2} - \frac{(q_1^2 + q_2^2)^6}{\Delta_3^3} \right] \mathcal{I}_1 \\ & - \frac{(q_1^2 - q_2^2) \log \frac{q_1^2}{q_2^2}}{64\pi q_1^2 w_1 \Delta_3} \left[\frac{5}{1024(q_1^2 w_1^2)^3} - \frac{3}{128(q_1^2 w_1^2)^2 \Delta_3} + \frac{1}{8q_1^2 w_1^2 \Delta_3^2} - \frac{1}{\Delta_3^3} \right] + \frac{\mathcal{I}_2}{\Delta_3^4}. \end{aligned} \quad (\text{C8})$$

Finally, a function with no SPs in either Δ_3 or in Π_1 is

$$I_2 = \frac{1}{\Pi_1^3} \left(\mathcal{I}_1 - \frac{(q_2^2)^2}{80\pi w_1^5} - \frac{11q_2^2}{240\pi w_1^3} - \frac{23}{240\pi w_1} \right). \quad (\text{C9})$$

I_1 and I_2 will render SP-free the part of the classical amplitude that is proportional to $m_1^3 m_2^2$. The combined transformations $q_1 \leftrightarrow q_2$ and $w_1 \leftrightarrow w_2$ yield the functions for the part of the amplitude that is proportional to $m_1^2 m_2^3$.

To expose the functions L_q , L_w , I_1 and I_2 in the expression of the amplitude, we use partial fractioning identities,²² to isolate the SPs in $\mathfrak{c}_{1,2}$, $\mathfrak{l}_{q,w,y}$ and \mathfrak{R} and further add and subtract appropriate combinations of logarithms and square roots. Their coefficients are, by construction, free of SPs. We then verified that the coefficients of the remaining logarithms are also free of SPs upon applying the Bianchi and four-dimensional identities. While all coefficients and rational terms are manifestly free of the initial SPs, this feature comes at the expense of introducing higher powers of the physical poles.

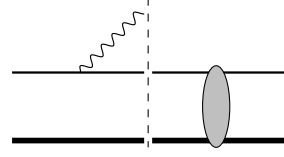


FIG. 3. The unitarity cut that only has support on the external zero energy graviton.

The final expressions are given in Eqs. (6.1) and (6.2) in the main text, and explicit expressions of the c and l coefficients there are included in the ancillary file `WaveformReorganisation.nb`.

Appendix D: Disconnected matrix elements supported by zero energy graviton

In this appendix, we will discuss the role of the cut contributions to \mathcal{M} that have support on the external zero energy graviton, which could potentially modify the constant background. Besides Fig. 1a that leads to the Schwarzschild background, other possible contributions

²² For this purpose we use the `Mathematica` package `MultivariateApart` [87].

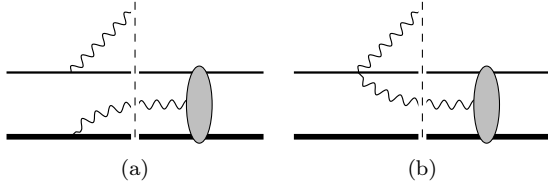


FIG. 4. The unitarity cuts that only have support when both the external and one internal graviton have zero energy.

to the background, given in Figs. 3 and 4, all involve a

cut.

We start with the cut in Fig. 3. It is more convenient here to use the true momenta of the massive particles. The cut is given by

$$S_5 = -i\kappa \left[(\varepsilon \cdot p_1)^2 \hat{\delta}(2p_1 \cdot k) + (1 \leftrightarrow 2) \right] \mathcal{M}_4. \quad (\text{D1})$$

We note that the true momentum p_a is related to p_a used in the main text through $p_a = p_a + q_a/2$. Since the unitarity cut forces the external graviton to have vanishing energy, it will interact with the five-point amplitude in the soft limit,

$$\begin{aligned} \mathcal{M}_5|_{\text{soft}} &= \kappa \left[-\frac{(\varepsilon \cdot p_1)^2}{2p_1 \cdot k + i\epsilon} - \frac{(\varepsilon \cdot p_2)^2}{2p_2 \cdot k + i\epsilon} + \frac{(\varepsilon \cdot p_3)^2}{2p_3 \cdot k - i\epsilon} + \frac{(\varepsilon \cdot p_4)^2}{2p_4 \cdot k - i\epsilon} \right] \mathcal{M}_4 \\ &= \kappa \left[i(\varepsilon \cdot p_1)^2 \hat{\delta}(2p_1 \cdot k) - \frac{2(\varepsilon \cdot p_1)(\varepsilon \cdot q_1) - (\varepsilon \cdot q_1)^2}{2p_1 \cdot k - i\epsilon} + \frac{(\varepsilon \cdot p_1 - \varepsilon \cdot q_1)^2}{2p_1 \cdot k - i\epsilon} \sum_{n=1}^{\infty} \left(\frac{2q_1 \cdot k}{2p_1 \cdot k - i\epsilon} \right)^n + (1 \leftrightarrow 2) \right] \mathcal{M}_4. \end{aligned} \quad (\text{D2})$$

We see that the delta functions cancel in the combination $\mathcal{M}_5 + S_5$ in the soft limit such that there are no contributions to the constant background. What is left is given in terms of retarded propagators. They will generate instead the memory at $t \rightarrow +\infty$. This statement works for more generic cases as we do not assume a particular loop order for \mathcal{M}_4 . In principle, the same conclusion can be drawn from using p_a momenta. The retarded matter propagators would then result from a cancellation between (derivatives of) delta functions and principal values, much like Ref. [42].

Finally, we sketch the derivation that the two cuts shown in Fig. 4 also vanish. For both cuts, we can use the soft limit of the five-point amplitude in the right blob

and sew it to the left blob. One will find that Fig. 4a only reduces to homogeneous integrands as in Eq. (5.18), which integrate to zero. For Fig. 4b, the only additional nontrivial integral is

$$\int d^d \ell \frac{\hat{\delta}(u_1 \cdot \ell) \hat{\delta}(u_2 \cdot k + u_2 \cdot \ell) \delta(\ell^2) \Theta(\ell^0)}{k \cdot \ell}. \quad (\text{D3})$$

One can rescale $\ell \rightarrow \omega \ell$ and find that the integral is proportional to $\omega^{d-4} \delta(\omega)$. However, because this integral comes from the diagram with a massless three-point vertex, signaled by the propagator $(k \cdot \ell)^{-1}$, the coefficient should scale as ω^2 . Therefore, overall we have the scaling $\omega^{d-2} \delta(\omega)$, which vanishes in four dimensions.

[1] **LIGO Scientific, Virgo** Collaboration, B. P. Abbott *et al.*, “Observation of Gravitational Waves from a Binary Black Hole Merger,” *Phys. Rev. Lett.* **116** no. 6, (2016) 061102, [arXiv:1602.03837 \[gr-qc\]](https://arxiv.org/abs/1602.03837).

[2] **LIGO Scientific, Virgo** Collaboration, B. P. Abbott *et al.*, “GW170817: Observation of Gravitational Waves from a Binary Neutron Star Inspiral,” *Phys. Rev. Lett.* **119** no. 16, (2017) 161101, [arXiv:1710.05832 \[gr-qc\]](https://arxiv.org/abs/1710.05832).

[3] D. A. Kosower, B. Maybee, and D. O’Connell, “Amplitudes, Observables, and Classical Scattering,” *JHEP* **02** (2019) 137, [arXiv:1811.10950 \[hep-th\]](https://arxiv.org/abs/1811.10950).

[4] A. Cristofoli, R. Gonzo, D. A. Kosower, and D. O’Connell, “Waveforms from amplitudes,” *Phys. Rev. D* **106** no. 5, (2022) 056007, [arXiv:2107.10193 \[hep-th\]](https://arxiv.org/abs/2107.10193).

[5] L. Blanchet and T. Damour, “Radiative gravitational fields in general relativity I. general structure of the field outside the source,” *Phil. Trans. Roy. Soc. Lond. A* **320** (1986) 379–430.

[6] L. Blanchet and T. Damour, “PostNewtonian Generation of Gravitational Waves,” *Ann. Inst. H. Poincaré Phys. Theor.* **50** (1989) 377–408.

[7] L. Blanchet, “Gravitational Radiation from Post-Newtonian Sources and Inspiralling Compact Binaries,” *Living Rev. Rel.* **17** (2014) 2, [arXiv:1310.1528 \[gr-qc\]](https://arxiv.org/abs/1310.1528).

[8] P. C. Peters, “Relativistic gravitational bremsstrahlung,” *Phys. Rev. D* **1** (1970) 1559–1571.

[9] S. J. Kovacs and K. S. Thorne, “The Generation of Gravitational Waves. 3. Derivation of Bremsstrahlung Formulas,” *Astrophys. J.* **217** (1977) 252–280.

[10] M. Portilla, “Scattering of Two Gravitating Particles: Classical Approach,” *J. Phys. A* **13** (1980) 3677–3683.

[11] K. Westpfahl, “High-Speed Scattering of Charged and

Uncharged Particles in General Relativity,” *Fortsch. Phys.* **33** no. 8, (1985) 417–493.

[12] Z. Bern, L. J. Dixon, D. C. Dunbar, and D. A. Kosower, “One loop n -point gauge theory amplitudes, unitarity and collinear limits,” *Nucl. Phys.* **B425** (1994) 217–260, [arXiv:hep-ph/9403226 \[hep-ph\]](https://arxiv.org/abs/hep-ph/9403226).

[13] Z. Bern and A. G. Morgan, “Massive loop amplitudes from unitarity,” *Nucl. Phys.* **B467** (1996) 479–509, [arXiv:hep-ph/9511336 \[hep-ph\]](https://arxiv.org/abs/hep-ph/9511336).

[14] Z. Bern, L. J. Dixon, D. C. Dunbar, and D. A. Kosower, “Fusing gauge theory tree amplitudes into loop amplitudes,” *Nucl. Phys.* **B435** (1995) 59–101, [arXiv:hep-ph/9409265 \[hep-ph\]](https://arxiv.org/abs/hep-ph/9409265).

[15] Z. Bern, L. J. Dixon, and D. A. Kosower, “One loop amplitudes for $e+e-$ to four partons,” *Nucl. Phys. B* **513** (1998) 3–86, [arXiv:hep-ph/9708239](https://arxiv.org/abs/hep-ph/9708239).

[16] R. Britto, F. Cachazo, and B. Feng, “Generalized unitarity and one-loop amplitudes in $N=4$ super-Yang-Mills,” *Nucl. Phys. B* **725** (2005) 275–305, [arXiv:hep-th/0412103](https://arxiv.org/abs/hep-th/0412103).

[17] Z. Bern, J. J. M. Carrasco, and H. Johansson, “New relations for gauge-theory amplitudes,” *Phys. Rev.* **D78** (2008) 085011, [arXiv:0805.3993 \[hep-ph\]](https://arxiv.org/abs/0805.3993).

[18] Z. Bern, J. J. M. Carrasco, and H. Johansson, “Perturbative quantum gravity as a double copy of gauge theory,” *Phys. Rev. Lett.* **105** (2010) 061602, [arXiv:1004.0476 \[hep-th\]](https://arxiv.org/abs/1004.0476).

[19] H. Kawai, D. C. Lewellen, and S. H. H. Tye, “A relation between tree amplitudes of closed and open strings,” *Nucl. Phys.* **B269** (1986) 1–23.

[20] K. G. Chetyrkin and F. V. Tkachov, “Integration by Parts: The Algorithm to Calculate beta Functions in 4 Loops,” *Nucl. Phys. B* **192** (1981) 159–204.

[21] S. Laporta, “High precision calculation of multiloop Feynman integrals by difference equations,” *Int. J. Mod. Phys. A* **15** (2000) 5087–5159, [arXiv:hep-ph/0102033](https://arxiv.org/abs/hep-ph/0102033).

[22] A. V. Smirnov, “Algorithm FIRE – Feynman Integral REduction,” *JHEP* **10** (2008) 107, [arXiv:0807.3243 \[hep-ph\]](https://arxiv.org/abs/0807.3243).

[23] A. V. Smirnov and F. S. Chuharev, “FIRE6: Feynman Integral REduction with Modular Arithmetic,” *Comput. Phys. Commun.* **247** (2020) 106877, [arXiv:1901.07808 \[hep-ph\]](https://arxiv.org/abs/1901.07808).

[24] A. V. Kotikov, “Differential equations method: New technique for massive Feynman diagrams calculation,” *Phys. Lett. B* **254** (1991) 158–164.

[25] Z. Bern, L. J. Dixon, and D. A. Kosower, “Dimensionally regulated pentagon integrals,” *Nucl. Phys. B* **412** (1994) 751–816, [arXiv:hep-ph/9306240](https://arxiv.org/abs/hep-ph/9306240).

[26] E. Remiddi, “Differential equations for Feynman graph amplitudes,” *Nuovo Cim. A* **110** (1997) 1435–1452, [arXiv:hep-th/9711188](https://arxiv.org/abs/hep-th/9711188).

[27] T. Gehrmann and E. Remiddi, “Differential equations for two loop four point functions,” *Nucl. Phys. B* **580** (2000) 485–518, [arXiv:hep-ph/9912329](https://arxiv.org/abs/hep-ph/9912329).

[28] G. Mogull, J. Plefka, and J. Steinhoff, “Classical black hole scattering from a worldline quantum field theory,” *JHEP* **02** (2021) 048, [arXiv:2010.02865 \[hep-th\]](https://arxiv.org/abs/2010.02865).

[29] G. Kälin and R. A. Porto, “Post-Minkowskian Effective Field Theory for Conservative Binary Dynamics,” *JHEP* **11** (2020) 106, [arXiv:2006.01184 \[hep-th\]](https://arxiv.org/abs/2006.01184).

[30] Z. Bern, J. Parra-Martinez, R. Roiban, M. S. Ruf, C.-H. Shen, M. P. Solon, and M. Zeng, “Scattering Amplitudes and Conservative Binary Dynamics at $\mathcal{O}(G^4)$,” *Phys. Rev. Lett.* **126** no. 17, (2021) 171601, [arXiv:2101.07254 \[hep-th\]](https://arxiv.org/abs/2101.07254).

[31] Z. Bern, J. Parra-Martinez, R. Roiban, M. S. Ruf, C.-H. Shen, M. P. Solon, and M. Zeng, “Scattering Amplitudes, the Tail Effect, and Conservative Binary Dynamics at $\mathcal{O}(G^4)$,” *Phys. Rev. Lett.* **128** no. 16, (2022) 161103, [arXiv:2112.10750 \[hep-th\]](https://arxiv.org/abs/2112.10750).

[32] C. Dlapa, G. Kälin, Z. Liu, and R. A. Porto, “Dynamics of binary systems to fourth Post-Minkowskian order from the effective field theory approach,” *Phys. Lett. B* **831** (2022) 137203, [arXiv:2106.08276 \[hep-th\]](https://arxiv.org/abs/2106.08276).

[33] G. U. Jakobsen, G. Mogull, J. Plefka, B. Sauer, and Y. Xu, “Conservative Scattering of Spinning Black Holes at Fourth Post-Minkowskian Order,” *Phys. Rev. Lett.* **131** no. 15, (2023) 151401, [arXiv:2306.01714 \[hep-th\]](https://arxiv.org/abs/2306.01714).

[34] G. U. Jakobsen, G. Mogull, J. Plefka, and B. Sauer, “Dissipative Scattering of Spinning Black Holes at Fourth Post-Minkowskian Order,” *Phys. Rev. Lett.* **131** no. 24, (2023) 241402, [arXiv:2308.11514 \[hep-th\]](https://arxiv.org/abs/2308.11514).

[35] G. U. Jakobsen, G. Mogull, J. Plefka, and J. Steinhoff, “Classical Gravitational Bremsstrahlung from a Worldline Quantum Field Theory,” *Phys. Rev. Lett.* **126** no. 20, (2021) 201103, [arXiv:2101.12688 \[gr-qc\]](https://arxiv.org/abs/2101.12688).

[36] S. Mougiakakos, M. M. Riva, and F. Vernizzi, “Gravitational Bremsstrahlung with Tidal Effects in the Post-Minkowskian Expansion,” *Phys. Rev. Lett.* **129** no. 12, (2022) 121101, [arXiv:2204.06556 \[hep-th\]](https://arxiv.org/abs/2204.06556).

[37] M. M. Riva, F. Vernizzi, and L. K. Wong, “Gravitational bremsstrahlung from spinning binaries in the post-Minkowskian expansion,” *Phys. Rev. D* **106** no. 4, (2022) 044013, [arXiv:2205.15295 \[hep-th\]](https://arxiv.org/abs/2205.15295).

[38] A. Elkhidir, D. O’Connell, M. Sergola, and I. A. Vazquez-Holm, “Radiation and Reaction at One Loop,” [arXiv:2303.06211 \[hep-th\]](https://arxiv.org/abs/2303.06211).

[39] A. Herderschee, R. Roiban, and F. Teng, “The sub-leading scattering waveform from amplitudes,” *JHEP* **06** (2023) 004, [arXiv:2303.06112 \[hep-th\]](https://arxiv.org/abs/2303.06112).

[40] A. Georgoudis, C. Heissenberg, and I. Vazquez-Holm, “Inelastic exponentiation and classical gravitational scattering at one loop,” *JHEP* **06** (2023) 126, [arXiv:2303.07006 \[hep-th\]](https://arxiv.org/abs/2303.07006).

[41] A. Brandhuber, G. R. Brown, G. Chen, S. De Angelis, J. Gowdy, and G. Travaglini, “One-loop gravitational bremsstrahlung and waveforms from a heavy-mass effective field theory,” *JHEP* **06** (2023) 048, [arXiv:2303.06111 \[hep-th\]](https://arxiv.org/abs/2303.06111).

[42] S. Caron-Huot, M. Giroux, H. S. Hannesdottir, and S. Mizera, “What can be measured asymptotically?,” [arXiv:2308.02125 \[hep-th\]](https://arxiv.org/abs/2308.02125).

[43] S. De Angelis, R. Gonzo, and P. P. Novichkov, “Spinning waveforms from KMOC at leading order,” [arXiv:2309.17429 \[hep-th\]](https://arxiv.org/abs/2309.17429).

[44] A. Brandhuber, G. R. Brown, G. Chen, J. Gowdy, and G. Travaglini, “Resummed spinning waveforms from five-point amplitudes,” [arXiv:2310.04405 \[hep-th\]](https://arxiv.org/abs/2310.04405).

[45] R. Aoude, K. Haddad, C. Heissenberg, and A. Helset, “Leading-order gravitational radiation to all spin orders,” [arXiv:2310.05832 \[hep-th\]](https://arxiv.org/abs/2310.05832).

[46] L. Bohnenblust, H. Ita, M. Kraus, and J. Schlenk, “Gravitational Bremsstrahlung in Black-Hole Scattering at $\mathcal{O}(G^3)$: Linear-in-Spin Effects,” [arXiv:2312.14859 \[hep-th\]](https://arxiv.org/abs/2312.14859).

[47] L. Blanchet, G. Faye, Q. Henry, F. Larrouturou, and D. Trestini, “Gravitational-Wave Phasing of Quasicircular Compact Binary Systems to the Fourth-and-a-Half Post-Newtonian Order,” *Phys. Rev. Lett.* **131** no. 12, (2023) 121402, [arXiv:2304.11185 \[gr-qc\]](https://arxiv.org/abs/2304.11185).

[48] L. Blanchet, G. Faye, Q. Henry, F. Larrouturou, and D. Trestini, “Gravitational-wave flux and quadrupole modes from quasicircular nonspinning compact binaries to the fourth post-Newtonian order,” *Phys. Rev. D* **108** no. 6, (2023) 064041, [arXiv:2304.11186 \[gr-qc\]](https://arxiv.org/abs/2304.11186).

[49] A. Einstein, “Über Gravitationswellen,” *Sitzungsber. Preuss. Akad. Wiss. Berlin (Math. Phys.)* **1918** (1918) 154–167.

[50] D. Bini, T. Damour, and A. Geralico, “Comparing one-loop gravitational bremsstrahlung amplitudes to the multipolar-post-Minkowskian waveform,” *Phys. Rev. D* **108** no. 12, (2023) 124052, [arXiv:2309.14925 \[gr-qc\]](https://arxiv.org/abs/2309.14925).

[51] A. Georgoudis, C. Heissenberg, and R. Russo, “An eikonal-inspired approach to the gravitational scattering waveform,” [arXiv:2312.07452 \[hep-th\]](https://arxiv.org/abs/2312.07452).

[52] G. Veneziano and G. A. Vilkovisky, “Angular momentum loss in gravitational scattering, radiation reaction, and the Bondi gauge ambiguity,” *Phys. Lett. B* **834** (2022) 137419, [arXiv:2201.11607 \[gr-qc\]](https://arxiv.org/abs/2201.11607).

[53] H. Bondi, M. G. J. van der Burg, and A. W. K. Metzner, “Gravitational waves in general relativity. 7. Waves from axisymmetric isolated systems,” *Proc. Roy. Soc. Lond. A* **269** (1962) 21–52.

[54] R. K. Sachs, “Gravitational waves in general relativity. 8. Waves in asymptotically flat space-times,” *Proc. Roy. Soc. Lond. A* **270** (1962) 103–126.

[55] T. Damour, “Radiative contribution to classical gravitational scattering at the third order in G ,” *Phys. Rev. D* **102** no. 12, (2020) 124008, [arXiv:2010.01641 \[gr-qc\]](https://arxiv.org/abs/2010.01641).

[56] T. Damour, “Analytical Calculations of Gravitational Radiation,” in *4th Marcel Grossmann Meeting on the Recent Developments of General Relativity*. 6, 1985.

[57] L. Kehrberger, “The case against smooth null infinity IV: Linearized gravity around Schwarzschild—an overview,” *Phil. Trans. Roy. Soc. Lond. A* **382** no. 2267, (2024) 20230039, [arXiv:2401.04170 \[gr-qc\]](https://arxiv.org/abs/2401.04170).

[58] T. Damour and N. Deruelle, “General relativistic celestial mechanics of binary systems. I. The post-Newtonian motion,” *Annales de L’Institut Henri Poincaré Section (A) Physique Théorique* **43** no. 1, (Jan., 1985) 107–132.

[59] T. Damour and G. Schaefer, “Higher Order Relativistic Periastron Advances and Binary Pulsars,” *Nuovo Cim. B* **101** (1988) 127.

[60] G. Cho, A. Gopakumar, M. Haney, and H. M. Lee, “Gravitational waves from compact binaries in post-Newtonian accurate hyperbolic orbits,” *Phys. Rev. D* **98** no. 2, (2018) 024039, [arXiv:1807.02380 \[gr-qc\]](https://arxiv.org/abs/1807.02380).

[61] L. Blanchet, “Energy losses by gravitational radiation in inspiraling compact binaries to five halves postNewtonian order,” *Phys. Rev. D* **54** (1996) 1417–1438, [arXiv:gr-qc/9603048](https://arxiv.org/abs/gr-qc/9603048). [Erratum: *Phys. Rev. D* **71**, 129904 (2005)].

[62] T. Damour and N. Deruelle, “Radiation Reaction and Angular Momentum Loss in Small Angle Gravitational Scattering,” *Phys. Lett. A* **87** (1981) 81.

[63] C. Cheung, I. Z. Rothstein, and M. P. Solon, “From Scattering Amplitudes to Classical Potentials in the Post-Minkowskian Expansion,” *Phys. Rev. Lett.* **121** no. 25, (2018) 251101, [arXiv:1808.02489 \[hep-th\]](https://arxiv.org/abs/1808.02489).

[64] Z. Bern, C. Cheung, R. Roiban, C.-H. Shen, M. P. Solon, and M. Zeng, “Black Hole Binary Dynamics from the Double Copy and Effective Theory,” *JHEP* **10** (2019) 206, [arXiv:1908.01493 \[hep-th\]](https://arxiv.org/abs/1908.01493).

[65] Z. Bern, C. Cheung, R. Roiban, C.-H. Shen, M. P. Solon, and M. Zeng, “Scattering Amplitudes and the Conservative Hamiltonian for Binary Systems at Third Post-Minkowskian Order,” *Phys. Rev. Lett.* **122** no. 20, (2019) 201603, [arXiv:1901.04424 \[hep-th\]](https://arxiv.org/abs/1901.04424).

[66] M. Beneke and V. A. Smirnov, “Asymptotic expansion of Feynman integrals near threshold,” *Nucl. Phys. B* **522** (1998) 321–344, [arXiv:hep-ph/9711391](https://arxiv.org/abs/hep-ph/9711391).

[67] R. Harlander, P. Kant, L. Mihaila, and M. Steinhauser, “Dimensional Reduction applied to QCD at three loops,” *JHEP* **09** (2006) 053, [arXiv:hep-ph/0607240](https://arxiv.org/abs/hep-ph/0607240).

[68] R. V. Harlander, D. R. T. Jones, P. Kant, L. Mihaila, and M. Steinhauser, “Four-loop beta function and mass anomalous dimension in dimensional reduction,” *JHEP* **12** (2006) 024, [arXiv:hep-ph/0610206](https://arxiv.org/abs/hep-ph/0610206).

[69] J. C. Collins, *Renormalization*, vol. 26 of *Cambridge Monographs on Mathematical Physics*. Cambridge University Press, Cambridge, 7, 2023.

[70] D. Bini, T. Damour, and A. Geralico, “Radiative contributions to gravitational scattering,” *Phys. Rev. D* **104** no. 8, (2021) 084031, [arXiv:2107.08896 \[gr-qc\]](https://arxiv.org/abs/2107.08896).

[71] S. Weinberg, “Infrared photons and gravitons,” *Phys. Rev.* **140** (1965) B516–B524.

[72] A. Luna, I. Nicholson, D. O’Connell, and C. D. White, “Inelastic Black Hole Scattering from Charged Scalar Amplitudes,” *JHEP* **03** (2018) 044, [arXiv:1711.03901 \[hep-th\]](https://arxiv.org/abs/1711.03901).

[73] J. Parra-Martinez, M. S. Ruf, and M. Zeng, “Extremal black hole scattering at $\mathcal{O}(G^3)$: graviton dominance, eikonal exponentiation, and differential equations,” *JHEP* **11** (2020) 023, [arXiv:2005.04236 \[hep-th\]](https://arxiv.org/abs/2005.04236).

[74] N. Craig, H. Elvang, M. Kiermaier, and T. Slatyer, “Massive amplitudes on the Coulomb branch of $N=4$ SYM,” *JHEP* **12** (2011) 097, [arXiv:1104.2050 \[hep-th\]](https://arxiv.org/abs/1104.2050).

[75] M. Kiermaier, “The Coulomb-branch S-matrix from massless amplitudes,” [arXiv:1105.5385 \[hep-th\]](https://arxiv.org/abs/1105.5385).

[76] M. J. Duff, “Quantum Tree Graphs and the Schwarzschild Solution,” *Phys. Rev. D* **7** (1973) .

[77] N. E. J. Bjerrum-Bohr, P. H. Damgaard, G. Festuccia, L. Planté, and P. Vanhove, “General Relativity from Scattering Amplitudes,” *Phys. Rev. Lett.* **121** no. 17, (2018) 171601, [arXiv:1806.04920 \[hep-th\]](https://arxiv.org/abs/1806.04920).

[78] A. Cristofoli, A. Elkhidir, A. Ilderton, and D. O’Connell, “Large gauge effects and the structure of amplitudes,” *JHEP* **06** (2023) 204, [arXiv:2211.16438 \[hep-th\]](https://arxiv.org/abs/2211.16438).

[79] T. Adamo, R. Gonzo, and A. Ilderton, “Gravitational Bound Waveforms from Amplitudes,” [arXiv:2402.00124 \[hep-th\]](https://arxiv.org/abs/2402.00124).

[80] Z. Bern, J. J. M. Carrasco, L. J. Dixon, H. Johansson, and R. Roiban, “Simplifying Multiloop Integrands and Ultraviolet Divergences of Gauge Theory and Gravity Amplitudes,” *Phys. Rev. D* **85** (2012) 105014, [arXiv:1201.5366 \[hep-th\]](https://arxiv.org/abs/1201.5366).

[81] S. Abreu, R. Britto, and H. Grönqvist, “Cuts and coproducts of massive triangle diagrams,” *JHEP* **07** (2015) 111, [arXiv:1504.00206 \[hep-th\]](https://arxiv.org/abs/1504.00206).

[82] J. L. Bourjaily, H. Hannesdottir, A. J. McLeod, M. D. Schwartz, and C. Vergu, “Sequential Discontinuities of Feynman Integrals and the Monodromy Group,” *JHEP* **01** (2021) 205, [arXiv:2007.13747 \[hep-th\]](https://arxiv.org/abs/2007.13747).

[83] F. Teng, “Understanding the NLO Scattering Waveform Soft Limit and Post-Newtonian Expansion.” Talk at QDC Meets Gravity IX, December, 2023.

[84] A. V. Manohar, A. K. Ridgway, and C.-H. Shen, “Radiated Angular Momentum and Dissipative Effects in Classical Scattering,” *Phys. Rev. Lett.* **129** no. 12, (2022) 121601, [arXiv:2203.04283 \[hep-th\]](https://arxiv.org/abs/2203.04283).

[85] P. Di Vecchia, C. Heissenberg, and R. Russo, “Angular momentum of zero-frequency gravitons,” *JHEP* **08** (2022) 172, [arXiv:2203.11915 \[hep-th\]](https://arxiv.org/abs/2203.11915).

[86] S. Abreu, J. Dormans, F. Febres Cordero, H. Ita, B. Page, and V. Sotnikov, “Analytic Form of the Planar Two-Loop Five-Parton Scattering Amplitudes in QCD,” *JHEP* **05** (2019) 084, [arXiv:1904.00945 \[hep-ph\]](https://arxiv.org/abs/1904.00945).

[87] M. Heller and A. von Manteuffel, “Multivariate Apart: Generalized partial fractions,” *Comput. Phys. Commun.* **271** (2022) 108174, [arXiv:2101.08283 \[cs.SC\]](https://arxiv.org/abs/2101.08283).

[88] R. Russo, “The Gravitational Eikonal and the NLO Scattering Waveform.” Talk at QDC Meets Gravity IX, December, 2023.

[89] B. Sahoo and A. Sen, “Classical soft graviton theorem rewritten,” *JHEP* **01** (2022) 077, [arXiv:2105.08739 \[hep-th\]](https://arxiv.org/abs/2105.08739).

[90] A. P. Saha, B. Sahoo, and A. Sen, “Proof of the classical soft graviton theorem in $D = 4$,” *JHEP* **06** (2020) 153, [arXiv:1912.06413 \[hep-th\]](https://arxiv.org/abs/1912.06413).

[91] A. Georgoudis, C. Heissenberg, and I. Vazquez-Holm, “More on the Subleading Gravitational Waveform,” [arXiv:2312.14710 \[hep-th\]](https://arxiv.org/abs/2312.14710).

[92] L. Bel, T. Damour, N. Deruelle, J. Ibanez, and J. Martin, “Poincaré-invariant gravitational field and equations of motion of two pointlike objects: The postlinear approximation of general relativity,” *Gen. Rel. Grav.* **13** (1981) 963–1004.

[93] S. Mougiakakos, M. M. Riva, and F. Vernizzi, “Gravitational Bremsstrahlung in the post-Minkowskian effective field theory,” *Phys. Rev. D* **104** no. 2, (2021) 024041, [arXiv:2102.08339 \[gr-qc\]](https://arxiv.org/abs/2102.08339).

[94] J. Ware, R. Saotome, and R. Akhoury, “Construction of an asymptotic S matrix for perturbative quantum gravity,” *JHEP* **10** (2013) 159, [arXiv:1308.6285 \[hep-th\]](https://arxiv.org/abs/1308.6285).

[95] L. Blanchet, A. Buonanno, and G. Faye, “Higher-order spin effects in the dynamics of compact binaries. II. Radiation field,” *Phys. Rev. D* **74** (2006) 104034, [arXiv:gr-qc/0605140](https://arxiv.org/abs/gr-qc/0605140). [Erratum: *Phys. Rev. D* 75, 049903 (2007), Erratum: *Phys. Rev. D* 81, 089901 (2010)].